Tomato receptor FLAGELLIN-SENSING 3 binds flgII-28 and activates the plant immune system

Sarah R. Hind[1], Susan R. Strickler[1], Patrick C. Boyle[1], Diane M. Dunham[1], Zhilong Bao[1], Inish M. O'Doherty[1,2], Joshua A. Baccile[1,2], Jason S. Hoki[1,2], Elise G. Viox[1], Christopher R. Clarke[3], Boris A. Vinatzer[3], Frank C. Schroeder[1,2], and Gregory B. Martin[1,4*]

[1]Boyce Thompson Institute for Plant Research, Ithaca, NY 14853, USA; [2]Department of Chemistry and Chemical Biology, Cornell University, Ithaca, NY 14853, USA; [3]Department of Plant Pathology, Physiology and Weed Sciences, Virginia Tech, Blacksburg, VA 24061, USA; [4]Section of Plant Pathology and Plant-Microbe Biology, School of Integrative Plant Science, Cornell University, Ithaca, NY 14853, USA; *indicates corresponding author

Abstract

Plants and animals detect the presence of potential pathogens through the perception of conserved microbial patterns by cell surface receptors. Certain solanaceous plants, including tomato, potato and pepper, detect flgII-28, a region of bacterial flagellin that is distinct from that perceived by the well-characterized FLS2 receptor. Here we identify and characterize the receptor responsible for this recognition in tomato, called FLAGELLIN-SENSING 3. This receptor binds flgII-28 and enhances immune responses leading to a reduction in bacterial colonization of leaf tissues. Further characterization of FLS3 and its signaling pathway could provide new insights into the plant immune system and transfer of the receptor to other crop plants offers the potential of enhancing resistance to bacterial pathogens that have evolved to evade FLS2-mediated immunity.

Introduction

The recognition of conserved microbe-associated molecular patterns (MAMPs) by pattern recognition receptors (PRRs) is one of the initial events that activates pattern-triggered immunity (PTI) in both plants and animals[1-4]. This immune response leads to the rapid generation of reactive oxygen species (ROS), activation of mitogen-associated protein kinases (MAPKs), and extensive changes in the transcriptome that together hinder the infection process[1,5,6]. The first plant PRR-MAMP pair, consisting of FLS2 and its ligand the flagellin epitope flg22, was identified 15 years ago, and works in concert with the co-receptor BAK1 to activate intracellular immune signaling[7,8,9,10]. Since then approximately 10 additional receptor-ligand pairs involved in immunity, either through perception of MAMPs or damage-associated molecular patterns (DAMPs), have been identified, with direct binding being demonstrated for only a subset of these pairs[2].

Recently, a subset of solanaceous species, including tomato, potato and pepper, but not *Nicotiana* spp., was found to recognize a second epitope of flagellin termed flgII-28[11,12]. FlgII-28 perception occurs independently of FLS2[12], but the molecular basis of its recognition is unknown. The discovery that tomato recognizes a second flagellin MAMP, combined with extensive natural variation and recent availability of the genome sequence for this species, offered the opportunity to identify the flgII-28 receptor using a genetic approach. Here, we use natural variation in tomato heirloom varieties and a mapping-by-sequencing approach to identify a receptor-like kinase gene, named *FLAGELLIN-SENSING 3* (*FLS3*), which confers responsiveness to flgII-28. We demonstrate that FLS3 is the flgII-28 receptor and show that FLS3-mediated immunity enhances resistance to a bacterial pathogen. FLS3 represents an orthogonal means for flagellin perception and therefore expression of this solanaceous-specific

PRR in crop plants that are normally unable to detect flgII-28 could be used to combat pathogens that have evolved to evade or subvert flg22 detection.

Results and Discussion

We previously reported natural variation for perception of flagellin epitopes among tomato heirloom varieties[13]. Further screening of ~100 accessions using an assay to detect ROS production identified 8 varieties and 2 tomato wild species accessions with a strongly reduced response to flgII-28 (Fig. 1a-b and Extended Data Fig. 1a-b). In order to identify the responsible gene by map-based cloning, segregating populations were generated by crossing accessions that are flgII-28 sensitive (LA1589 and Rio Grande) or insensitive (Yellow Pear, Matt's Wild Cherry and Galapagos). The resulting F1 plants were responsive to flgII-28 (Extended Data Fig. 1c-d), indicating the allele responsible for the sensitivity is dominant. Testing of F2 plants with the ROS assay revealed a segregation ratio of 3:1 (sensitive:insensitive) in two of the three populations (Extended Data Fig. 1e) indicating that flgII-28 sensitivity can be conferred by a simply-inherited locus.

To identify the genomic region linked to flgII-28 sensitivity, we generated DNA libraries for next-generation Illumina sequencing using flgII-28 non-responsive F2 plants from the LA1589 x Yellow Pear cross because genome sequences were available for these lines. Analysis of the sequencing data showed that only chromosome 4 had a notable deviation from the expected 1:1 LA1589:Yellow Pear SNP ratio (Extended Data Fig. 2), with one region in particular having very few LA1589-specific SNPs. This region, spanning 2.619 to 5.486 Mb from the end of the chromosome, contains 322 annotated genes including 9 leucine-rich repeat, receptor-like kinases (LRR-RLKs).

In parallel, we analyzed SNP data generated independently from 75 tomato cultivars[14]. Relationships among the varieties based on genome-wide SNPs revealed no similarity among three known flgII-28 insensitive cultivars (Yellow Pear, Gold Ball Livingston, and San Marzano). A separate analysis using only SNPs between 1 and 10 Mb on chromosome 4 identified a close relationship of the insensitive cultivars (Extended Data Fig. 3). These analyses further supported this region as the location of the flgII-28 sensitivity locus.

We next performed fine mapping using DNA markers and succeeded in delimiting a <0.6 Mb region that co-segregated with flgII-28 sensitivity (Extended Data Table 1); this region contained one receptor-like kinase gene (*Solyc04g009640*), which we tentatively designated *FLAGELLIN-SENSITIVE 3* (*FLS3*) (Fig. 1c). We confirmed that this region was linked to the sensitive phenotype observed in our other two segregating F2 populations (Extended Data Figure 1f). Analysis of *FLS3* in non-responding accessions identified two alleles that were different from the allele in the flgII-28-responsive accessions Heinz1706, Rio Grande and LA1589. Remarkably, one of these alleles, *fls3-1*, was present in 8 insensitive tomato cultivars and one *S. pimpinellifolium* accession; this allele has a single nucleotide deletion that causes an aberrant stop codon (Fig. 1d, Extended Data Table 2 and Extended Data Fig. 4a). The other allele, *fls3-2*, was found in one accession of *S. pimpinellifolium* and encodes a full-length protein with four amino acid changes (Fig. 1d, Extended Data Table 2 and Extended Data Fig. 4a).

The expression of many PRR-encoding genes is induced by MAMPs[15]. Using available RNA sequencing data (Rosli *et al*.[6] and Tomato Functional Genomics Database, http://ted.bti.cornell.edu/), we found that expression of *FLS3* is induced by flg22 and flgII-28 treatment similar to that observed for *FLS2.1* (Extended Data Fig. 1g). The tomato bacterial pathogen *Pseudomonas syringae* pv. *tomato* DC3000 (*Pst* DC3000) has two well-characterized

effector proteins, AvrPto and AvrPtoB, which are known to suppress PTI-related immune responses, including the induction of PTI-related gene expression[16]. Similar to *FLS2.1*, transcript abundance of *FLS3* increased after inoculation with a *Pst* DC3000 strain that lacks *avrPto* and *avrPtoB* (Δ*avrPto*Δ*avrPtoB*), and this increase was inhibited by *Pst* DC3000, indicative of effector suppression (Extended Data Fig. 1g). Thus, *FLS3* belongs to a subset of tomato genes referred to as *FIRE* genes (*Flagellin-induced, repressed by effectors*)[6].

The *FLS3* gene encodes a class XII RLK[17] with 27 LRRs although it lies in a sub-clade of this class that is distinct from EFR, FLS2, and XA21[17]. Typical of many immune receptors[18], FLS3 has a non-RD intracellular kinase domain (Extended Data Fig. 4a). We identified potential *FLS3* orthologs from sequenced accessions of potato and pepper, but not from *Nicotiana benthamiana* or petunia (Extended Data Fig. 4b). Certain varieties of pepper and potato were previously shown to be sensitive to flgII-28[12] and we found the sequenced accessions were also sensitive, whereas *Nicotiana benthamiana* and petunia are not (data not shown and Extended Data Fig. 4c-d). These observations suggest that the *FLS3* gene likely arose, possibly by duplication of a related gene, after the divergence of *Capsicum* and *Solanum* from other solanaceous species.

The strong selection for weakly immunogenic flgII-28 alleles in *Pst* field populations, which originally led to the identification of this MAMP[11], is compelling evidence of its importance in natural plant-bacterial interactions. In order to investigate whether flgII-28 plays a role in tomato resistance to *Pseudomonas* strains under controlled laboratory conditions, we utilized the pathogen *Pseudomonas cannabina* pv. *alisalensis* ES4326 (*Pcal* ES4326; formerly *P.s. maculicola*[12]) which has a flg22 sequence that is not recognized by tomato[12] but a flgII-28 which is recognized (Fig. 2a-b). We used this pathogen because it allowed us to specifically test the

contribution of flgII-28 perception to plant immunity independent of flg22 recognition by FLS2. *Pcal* ES4326 grew to higher levels and caused more severe disease symptoms in LA1589 x Yellow Pear F2 plants that lacked *FLS3* (i.e., *fls3-1/fls3-1*) compared to F2 plants with *FLS3* (i.e., *FLS3/FLS3* or *FLS3/fls3-1*) (Extended Data Fig. 5a-b), suggesting that the presence of *FLS3* confers recognition of this bacterial pathogen and leads to modest disease resistance.

To further test whether this difference in bacterial growth was due to flgII-28 recognition, we developed a PTI induction assay in which we used heat-killed *Pst* strains expressing *fliC* variants from either *Pst* DC3000 (i.e., in which both flg22 and flgII-28 are active) or *Pcal* ES4326 (i.e. in which only flgII-28 is active) as a source of flagellin. We first induced PTI by infiltrating this solution into plants and then challenged them 16 hours later with a virulent bacterial pathogen, either a *Pst* strain lacking flagellin or *Pcal* ES4326. We used LA1589 and Yellow Pear to test this system and observed that the plants pretreated with heat-killed DC3000 *fliC* had significantly less bacterial growth and symptom production compared to those pretreated with the empty vector control (Fig. 2c and Extended Data Fig. 5c), likely due to PTI induction by FLS2 recognition of flg22. However, for plants pretreated with heat-killed ES4326 *fliC*, only LA1589 plants had significantly less bacterial growth compared to the empty vector control (Fig. 2c and Extended Data Fig. 5c), suggesting that since Yellow Pear lacks *FLS3*, it does not recognize the flgII-28 epitope of the ES4326 flagellin protein. Subsequently, we tested the F2 plants segregating for *FLS3* and *fls3-1*, and observed that pretreatment using heat-killed ES4326 *fliC* led to significant differences in bacterial growth depending on the genotype of the plants. Plants that lacked *FLS3* (i.e., *fls3-1/fls3-1*) showed higher bacterial growth and more severe symptoms similar to the Yellow Pear parent as compared to F2 plants that had at least one copy of *FLS3* (i.e., *FLS3/FLS3* or *FLS3/fls3-1*) or to LA1589 (Fig. 2d-e). These differences were not

observed when the plants were pretreated with heat-killed DC3000 *fliC* (Extended Data Fig. 5d-e), suggesting that the observed bacterial virulence differences are attributable to PTI induction by FLS3 perception of flgII-28.

To determine if ectopic expression of FLS3 is able to confer flgII-28 sensitivity, we transfected Yellow Pear protoplasts with an *FLS3* construct and tested for phosphorylation of MAPK proteins, which occurs in the responsive Rio Grande cultivar upon flgII-28 treatment (Fig. 3a). Expression of FLS3 resulted in an increase of phosphorylated MAPKs specifically after flgII-28 treatment, similar to levels observed either with the control treatment flg22, or with expression of the unrelated PRR EFR and treatment with its cognate ligand elf18 (Fig. 3a). Treatment of FLS3-expressing protoplasts with elf18 did not cause MAPK activation, indicating the response to flgII-28 treatment was specific. Transient expression of FLS3 in normally insensitive *N. benthamiana* leaves followed by treatment with flgII-28 resulted in production of ROS (Fig. 3b and Extended Data Fig. 6a). As a control, we showed that treatment with flgII-28 in leaves expressing YFP did not induced ROS production compared to the water controls, (Fig. 3b).

To gain insight into whether kinase activity of FLS3 is involved in the flgII-28-mediated response, we generated an *FLS3* variant encoding a protein with a K877Q substitution in the ATP binding site (see Extended Data Fig. 4a). This K residue, which is responsible for phosphotransfer[19], is required for downstream signaling events in other plant PRRs[5,20]. FLS3(K877Q) protein accumulated in *N. benthamiana* leaves the same as wild-type FLS3 (Extended Data Fig. 6b), however the ROS production measured after flgII-28 treatment was similar to that produced by the water control (Fig. 3c). The *fls3-2* allele present in LA1279 has a T1011P substitution in the kinase P+1 loop (Extended Data Fig. 4a) and we hypothesized this

change might also reduce the response of FLS3 to flgII-28. We observed a reduction in the ROS response of FLS3(T1011P) to flgII-28, while the protein accumulation was unaltered (Fig. 3c and Extended Data Fig. 6b). To confirm this substitution is responsible for the reduced flgII-28 sensitivity of LA1279, we expressed FLS3-2 in *N. benthamiana* leaves and observed reduced ROS production after flgII-28 treatment compared to wild-type FLS3 (Fig. 3d). Importantly, introduction of a P1011T substitution into FLS3-2 restored flgII-28 sensitivity to wild-type levels, while the protein accumulation remained equal for all proteins (Fig. 3d and Extended Data Fig. 6c). Although these results suggest that kinase activity is important for FLS3 signaling, we have been unable to detect *in vitro* or *in vivo* kinase activity for FLS3 (similar to a recent report for FLS2 activity[20]) and so it is presently unknown whether these substitutions affect enzymatic properties or alter interactions with signaling components independent of kinase activity.

To investigate if flgII-28 directly and specifically binds FLS3, we developed a photo-affinity labeling strategy similar to that used to demonstrate direct binding of brassinosteroids to the BRI1 receptor[21]. Synthetic samples of the flgII-28 and flg22 peptides were converted into photo-affinity probes flgII-28* and flg22*, respectively via selective addition of a bifunctional chemical tag to the *N*-terminal amine of each peptide (see Supplemental Methods). This chemical tag includes a methyl trifluorodiazirine photo-crosslinker moiety, enabling UV-irradiation triggered covalent attachment of the peptide probe to its cognate PRR, in addition to an alkyne handle, permitting installation of a biotin reporter tag via 'click chemistry' (Fig. 4a). Importantly, the modified peptide probes, flgII-28* and flg22*, retained the ability to elicit an immune response (Extended Data Fig. 7a-e).

Next, we treated purified plasma membrane preparations from *N. benthamiana* leaves expressing FLS3-GFP with flgII-28* or flg22* and subsequently UV-irradiated for photo-crosslinking (Extended Data Fig. 7f). FLS3-GFP was then immunoprecipitated using the GFP tag and subsequently biotinylated via click chemistry. Only plasma membranes treated with flgII-28*, but not those treated with flg22*, showed FLS3-GFP biotinylation (Fig. 4b), demonstrating the affinity of FLS3 for flgII-28*. In parallel, we performed the same experiment using FLS2-GFP, and only observed FLS2-GFP biotinylation when samples were treated with flg22* but not with flgII-28*. In addition to demonstrating that FLS3 is the receptor for flgII-28, these data establish the specificity of peptide-probe binding and UV-crosslinking between the ligands and their cognate receptors.

In order to determine the specific affinity of FLS3 for flgII-28, a series of flgII-28* concentrations was used for binding and crosslinking; FLS3-flgII-28* complexes were clearly detected at low nanomolar concentrations of flgII-28* (Fig. 4c). Binding could also be weakly observed at sub-nanomolar concentrations, but only when the blots were exposed for a long period (i.e., one hour compared to less than 10 minutes; for comparison the exposures for the anti-GFP blots to demonstrate equal loading were equivalent at 1 minute each between the left and right panels of Fig. 4c). We performed similar experiments for flg22* binding to FLS2, and observed binding consistently at 50 nM flg22* (Fig. 4d). This concentration is higher than the EC50 value of ~0.03 nM that was reported previously[22].This could be due to the propensity of flg22 to stick to surfaces[23]; during purification of flg22* we observed that addition of the hydrophobic crosslinking moiety further increased this tendency to surface deposit and aggregate.

We observed that simultaneous treatment of flgII-28* with a large excess (40-fold) of unmodified flgII-28 eliminated biotinylation of FLS3-GFP, indicating that these two peptides compete for the same binding site (Fig. 4e). When decreasing concentrations (i.e., 20-fold to 0.4-fold) of unmodified flgII-28 were added, the amount of biotinylated FLS3-GFP increased (Fig. 4e). As expected, treatment with flgII-28* and a 40-fold excess of flg22 did not prevent biotinylation of FLS3-GFP, indicating that flg22 does not compete with flgII-28* in binding to FLS3-GFP (Fig. 4e). Collectively, these results show that FLS3 binds directly and specifically to flgII-28 and represents a *bona fide* receptor of this ligand.

To gain further insight into FLS3 signaling, we investigated whether the co-receptor BAK1 (also known as NbSERK3 in *N. benthamiana*[10]) was necessary for flgII-28 responsiveness as it is for both FLS2 and EFR signaling[9,10,24]. Since we were unable to detect FLS3 protein accumulation in either transfected *Arabidopsis* protoplasts or stably transformed *Arabidopsis* plants (data not shown), we instead used *N. benthamiana* plants knocked down for *BAK1* expression by virus-induced gene silencing (VIGS). Silencing of *BAK1* was confirmed by quantitative RT-PCR (Extended Data Fig. 8a) and we observed significantly reduced ROS production upon flgII-28 treatment in *BAK1*-silenced leaves expressing FLS3 compared to control-silenced plants (Fig. 5a), though FLS3 protein accumulation was comparable (Extended Data Fig. 6d). Overexpression of Arabidopsis BAK1 along with FLS3 in *BAK1*-silenced plants increased ROS production upon flgII-28 treatment (Extended Data Fig. 8b).

We next investigated whether FLS3 and BAK1 could physically associate in plant cells, and whether this interaction was ligand-dependent as is the case for the FLS2-BAK1 interaction[25]. Epitope-tagged versions of each protein were co-expressed in *N. benthamiana* leaves using agroinfiltration; the infiltrated areas were treated either with solutions of 1 μM flgII-28 or flg22

peptides or buffer alone prior to harvesting, and the proteins were immunoprecipitated for analysis by immunoblotting. FLS3 co-immunoprecipitated with BAK1 specifically in the presence of flgII-28, similar to FLS2 though a small amount of flg22-independent interaction between FLS2 and BAK1 could be observed, possibly due to the better expression of FLS2 protein in the samples (Fig. 5b and Extended Data Fig. 8c). This interaction was specific, as the YFP control could not pull down FLS3 (Extended Data Fig. 8d). Collectively, these data indicate that FLS3 signaling occurs through a BAK1-dependent mechanism.

Finally, to reveal possible connections with the known PTI suppression activities of pathogen effectors, we investigated whether the *Pst* effector proteins AvrPto and AvrPtoB, which suppress FLS2- and EFR-mediated signaling[16], also suppress FLS3 signaling. Co-expression of AvrPto with FLS3 in *N. benthamiana* leaves caused a reduction in ROS production after flgII-28 treatment (Fig. 5c). Similar results were obtained with co-expression of $AvrPtoB_{1-387}$, which lacks the effector E3 ligase domain[26] (Fig. 5d); accumulation of FLS3 protein was not substantially altered in the presence of either effector (Extended Data Figure 6e-f). These results demonstrate that the effectors target FLS3 signaling, although the specific mechanisms of suppression remain to be investigated.

The discovery that FLS3 acts in addition to FLS2 to detect flagellin represents a pioneering example in plants where two receptors have been identified which recognize different MAMPs within the same pathogen protein[11,12]. However, this phenomenon has been reported in mammals, where extracellular TLR5 and intracellular NAIP5/6 receptors perceive different epitopes of flagellin[27,28]. The presence of multiple MAMPs within the same microbial feature may not be unique to flagellin, because it was recently reported that an epitope of EF-Tu in a

252 region distinct from elf18, called EFa50, is able to induce PTI responses in rice[29]; however, the
253 receptor for the second EF-Tu MAMP is unknown.
254 FLS3 and FLS2 belong to divergent sub-clades of class XII RLKs[17] and it is possible that,
255 despite their mutual dependence on BAK1, the two receptors act with some different host
256 components to promote PTI. This possibility might explain why FLS3 causes a more sustained
257 production of ROS than does FLS2 in response to their respective ligands (e.g., Fig. 1a). It is
258 unknown to what extent FLS3 and FLS2 might contribute additively or redundantly to the host
259 response to flagellin-derived MAMPs. This question is addressable by generating in the same
260 genetic background single and double mutants in the receptor genes using CRISPR technology.
261 Given the difference between flg22 and flgII-28 and in the LRR domains of the receptors, it
262 seems likely that FLS3 binds flgII-28 in a manner distinct from FLS2. Future comparisons of
263 FLS3 and FLS2 have the potential to reveal new insights into the evolution, structural biology,
264 and mechanisms underlying PTI in tomato.
265 There are several mechanisms by which bacteria evade recognition of their flagellin. One
266 tactic deployed by several *Pseudomonas* spp. involves degradation of excess flagellin monomers
267 by an alkaline protease secreted from the bacteria[30,31]. Another more broadly employed strategy
268 is the attenuation of flagellin recognition through the alteration of MAMPs important for
269 recognition by a host receptor[32]. There are now several reports of the transfer of PRRs from one
270 plant species to another conferring broadened resistance to pathogens[33-40]. Therefore, it is
271 possible that FLS3 could be used in the development of plants which have resistance against
272 bacterial pathogens that have evolved to evade recognition of their flg22 region; *Pcal* ES4326 is
273 one example of such a bacterium. In addition, some heirloom tomato varieties are known to
274 generate very high levels of ROS in response to flgII-28[13]) and it is possible that such genetic

variation might be useful in the breeding of cultivars with enhanced resistance to bacterial pathogens.

References

1. Boller, T. & Felix, G. A renaissance of elicitors: perception of microbe-associated molecular patterns and danger signals by pattern-recognition receptors. *Annu Rev Plant Biol* **60**, 379-406 (2009).

2. Zipfel, C. Plant pattern-recognition receptors. *Trends Immunol* **35**, 345-51 (2014).

3. O'Neill, L.A., Golenbock, D. & Bowie, A.G. The history of Toll-like receptors - redefining innate immunity. *Nat Rev Immunol* **13**, 453-60 (2013).

4. Rossez, Y., Wolfson, E.B., Holmes, A., Gally, D.L. & Holden, N.J. Bacterial flagella: twist and stick, or dodge across the kingdoms. *PLoS Pathog* **11**, e1004483 (2015).

5. Asai, T. *et al.* MAP kinase signalling cascade in *Arabidopsis* innate immunity. *Nature* **415**, 977-83 (2002).

6. Rosli, H.G. *et al.* Transcriptomics-based screen for genes induced by flagellin and repressed by pathogen effectors identifies a cell wall-associated kinase involved in plant immunity. *Genome Biol* **14**, R139 (2013).

7. Sun, Y. *et al.* Structural basis for flg22-induced activation of the *Arabidopsis* FLS2-BAK1 immune complex. *Science* **342**, 624-8 (2013).

8. Gomez-Gomez, L. & Boller, T. FLS2: an LRR receptor-like kinase involved in the perception of the bacterial elicitor flagellin in *Arabidopsis*. *Mol Cell* **5**, 1003-11 (2000).

9. Chinchilla, D. *et al.* A flagellin-induced complex of the receptor FLS2 and BAK1 initiates plant defence. *Nature* **448**, 497-500 (2007).

10. Heese, A. *et al.* The receptor-like kinase SERK3/BAK1 is a central regulator of innate immunity in plants. *Proc Natl Acad Sci USA* **104**, 12217-22 (2007).

11. Cai, R. *et al.* The plant pathogen *Pseudomonas syringae* pv. *tomato* is genetically monomorphic and under strong selection to evade tomato immunity. *PLoS Pathog* **7**, e1002130 (2011).

12. Clarke, C.R. *et al.* Allelic variation in two distinct *Pseudomonas syringae* flagellin epitopes modulates the strength of plant immune responses but not bacterial motility. *New Phytol* **200**, 847-60 (2013).

13. Veluchamy, S., Hind, S.R., Dunham, D.M., Martin, G.B. & Panthee, D.R. Natural variation for responsiveness to flg22, flgII-28, and csp22 and *Pseudomonas syringae* pv. *tomato* in heirloom tomatoes. *PLoS One* **9**, e106119 (2014).

14. Sim, S.C. *et al.* High-density SNP genotyping of tomato (*Solanum lycopersicum* L.) reveals patterns of genetic variation due to breeding. *PLoS One* **7**, e45520 (2012).

15. Zipfel, C. *et al.* Perception of the bacterial PAMP EF-Tu by the receptor EFR restricts *Agrobacterium*-mediated transformation. *Cell* **125**, 749-60 (2006).

16. Martin, G.B. Suppression and activation of the plant immune system by *Pseudomonas syringae* effectors AvrPto and AvrPtoB. in *Effectors in Plant-Microbe Interactions* (eds. Martin, F. & Kamoun, S.) 123-154. (Wiley-Blackwell, 2012).

17. Andolfo, G. *et al.* Overview of tomato (*Solanum lycopersicum*) candidate pathogen recognition genes reveals important *Solanum* R locus dynamics. *New Phytol* **197**, 223-37 (2013).

18. Dardick, C., Schwessinger, B. & Ronald, P. Non-arginine-aspartate (non-RD) kinases are associated with innate immune receptors that recognize conserved microbial signatures. *Curr Opin Plant Biol* **15**, 358-66 (2012).

19. Carrera, A.C., Alexandrov, K. & Roberts, T.M. The conserved lysine of the catalytic domain of protein kinases is actively involved in the phosphotransfer reaction and not required for anchoring ATP. *Proc Natl Acad Sci USA* **90**, 442-6 (1993).

20. Schwessinger, B. *et al.* Phosphorylation-dependent differential regulation of plant growth, cell death, and innate immunity by the regulatory receptor-like kinase BAK1. *PLoS Genet* **7**, e1002046 (2011).

21. Kinoshita, T. *et al.* Binding of brassinosteroids to the extracellular domain of plant receptor kinase BRI1. *Nature* **433**, 167-71 (2005).

22. Bauer, Z., Gomez-Gomez, L., Boller, T. & Felix, G. Sensitivity of different ecotypes and mutants of Arabidopsis thaliana toward the bacterial elicitor flagellin correlates with the presence of receptor-binding sites. *J Biol Chem* **276**, 45669-76 (2001).

23. Mueller, K. *et al.* Contamination risks in work with synthetic peptides: flg22 as an example of a pirate in commercial peptide preparations. *Plant Cell* **24**, 3193-7 (2012).

24. Roux, M. *et al.* The *Arabidopsis* leucine-rich repeat receptor-like kinases BAK1/SERK3 and BKK1/SERK4 are required for innate immunity to hemibiotrophic and biotrophic pathogens. *Plant Cell* **23**, 2440-55 (2011).

25. Schulze, B. *et al.* Rapid heteromerization and phosphorylation of ligand-activated plant transmembrane receptors and their associated kinase BAK1. *J Biol Chem* **285**, 9444-51 (2010).

26. Xiao, F. *et al.* The N-terminal region of *Pseudomonas* type III effector AvrPtoB elicits Pto-dependent immunity and has two distinct virulence determinants. *Plant J* **52**, 595-614 (2007).

27. Broz, P. & Monack, D.M. Newly described pattern recognition receptors team up against intracellular pathogens. *Nat Rev Immunol* **13**, 551-65 (2013).

28. Lage, S.L. *et al.* Emerging concepts about NAIP/NLRC4 inflammasomes. *Front Immunol* **5**, 309 (2014).

29. Furukawa, T., Inagaki, H., Takai, R., Hirai, H. & Che, F.S. Two distinct EF-Tu epitopes induce immune responses in rice and *Arabidopsis*. *Mol Plant Microbe Interact* **27**, 113-24 (2014).

30. Bardoel, B.W. *et al. Pseudomonas* evades immune recognition of flagellin in both mammals and plants. *PLoS Pathog* **7**, e1002206 (2011).

31. Pel, M.J. *et al. Pseudomonas syringae* evades host immunity by degrading flagellin monomers with alkaline protease AprA. *Mol Plant Microbe Interact* **27**, 603-10 (2014).

32. Vinatzer, B.A., Monteil, C.L. & Clarke, C.R. Harnessing population genomics to understand how bacterial pathogens emerge, adapt to crop hosts, and disseminate. *Annu Rev Phytopathol* **52**, 19-43 (2014).

33. Lacombe, S. *et al.* Interfamily transfer of a plant pattern-recognition receptor confers broad-spectrum bacterial resistance. *Nat Biotechnol* **28**, 365-9 (2010).

34. Tripathi, J.N., Lorenzen, J., Bahar, O., Ronald, P. & Tripathi, L. Transgenic expression of the rice *Xa21* pattern-recognition receptor in banana (*Musa* sp.) confers resistance to *Xanthomonas campestris* pv. *musacearum*. *Plant Biotechnol J* **12**, 663-73 (2014).

35. Afroz, A. *et al.* Enhanced resistance against bacterial wilt in transgenic tomato (*Lycopersicon esculentum*) lines expressing the *Xa21* gene. *Plant Cell Tiss Organ Cult* **104**, 227-237 (2011).

366 36. Mendes, B.M.J. *et al.* Reduction in susceptibility to *Xanthomonas axonopodis* pv. *citri* in
367 transgenic *Citrus sinensis* expressing the rice *Xa21* gene. *Plant Path* **59**, 68-75 (2010).

368 37. Holton, N., Nekrasov, V., Ronald, P.C. & Zipfel, C. The phylogenetically-related pattern
369 recognition receptors EFR and XA21 recruit similar immune signaling components in
370 monocots and dicots. *PLoS Pathog* **11**, e1004602 (2015).

371 38. Lu, F. *et al.* Enhancement of innate immune system in monocot rice by transferring the
372 dicotyledonous elongation factor Tu receptor EFR. *J Integr Plant Biol* **57**, 641-52 (2015).

373 39. Schoonbeek, H.J. *et al. Arabidopsis* EF-Tu receptor enhances bacterial disease resistance in
374 transgenic wheat. *New Phytol* **206**, 606-13 (2015).

375 40. Schwessinger, B. *et al.* Transgenic expression of the dicotyledonous pattern recognition
376 receptor EFR in rice leads to ligand-dependent activation of defense responses. *PLoS Pathog*
377 **11**, e1004809 (2015).

378

379 **Supplementary information** is linked to the online version of the paper at

380 www.nature.com/nature.

381

382 **Acknowledgments** We thank Esther van der Knapp for providing tomato seeds, Hai-Lei Wei for
383 DC3000 strains, John Debbie for assistance with analysis of the *FLS3* sequences from various
384 tomato cultivars, Christine Kraus and Simon Schwizer for testing *FLS3* expression in
385 *Arabidopsis thaliana*, Simon Schwizer and Johannes Mathieu for DNA constructs, and Simon
386 Schwizer for proofreading. This research was supported by grants from the National Science
387 Foundation to G.B.M. (IOS-1025642) and B.A.V. (IOS-1354215), the USDA-National Initiative
388 in Food and Agriculture (2010-65108-20503) to G.B.M., the USDA Binational Agriculture
389 Development Fund (IS-4510-12C) to G.B.M., and the National Institutes of Health (R01-
390 GM078021) to G.B.M.; by the TRIAD foundation to G.B.M. and F.C.S.; by a Postdoctoral
391 Fellowship from the Human Frontiers Science Program to P.C.B.; by a summer REU stipend to

E.G.V. (National Science Foundation REU Site award DBI-1358843); and by internal funding from the Boyce Thompson Institute to S.R.S.

Author Contributions S.R.H. and G.B.M. conceived, designed, and analyzed, while S.R.H. performed the experiments except as noted below. S.R.S. designed and performed the bioinformatics analyses, and assisted with primer design. D.M.D. performed some of the experiments shown in Figures 2 and 3, Extended Data Figures 5 and 8. P.C.B., I.M.O., and J.A.B. conceived and designed the experiments shown in Figure 4 and Extended Data Figure 7. Z.B. cloned, sequenced and analyzed the *FLS3* genomic sequences from tomato cultivars and *S. pimpinellifolium* accessions. E.G.V. performed the experiments shown in Figure 2a-b. I.M.O., J.A.B. and F.C.S. provided technical assistance and advice in the development and application of crosslinking and click chemistry conditions, and I.M.O., J.A.B., and J.S.H. designed and synthesized the chemistries needed for the peptide probe generation. B.A.V. and C.R.C. designed, and C.R.C. performed the experiments in Extended Data Figure 1d-f. S.R.H. and G.B.M. wrote the manuscript with input from all co-authors.

Author Information Sequences were submitted to NCBI as project number PRJNA263381. Data and output from this study can be accessed through the Solgenomics ftpsite: ftp://ftp.solgenomics.net/. Reprints and permissions information is available at www.nature.com/reprints. The authors declare no competing financial interests. Correspondence and request for materials should be addressed to G.B.M. (gbm7@cornell.edu).

Figure 1. flgII-28 responsiveness is associated with a region on Chromosome 4 in tomato. **a, b,** Oxidative burst produced by *S. pimpinellifolium* LA1589 (**a**) or *S. lycopersicum* cv. 'Yellow Pear' (**b**) leaves treated with 100 nM flg22 or flgII-28, or with water, and measured in relative light units (RLU). Results shown are means ± s.d. (n = 4 plants). Similar results were obtained in three independent experiments. **c,** Fine mapping of the chromosome 4 region associated with flgII-28 sensitivity. Marker positions are indicated by the vertical black bars, and the number of plants showing recombination (# recomb.) is indicated. The approximate locations of 9 LRR-RLK genes are indicated by horizontal bars. **d,** Mutant allele deletions and SNPs are indicated on the gene model of *FLS3* (*Solyc04g009640*).

Figure 2. FLS3 is associated with enhanced resistance to bacterial infection. a, b, Oxidative burst produced by *S. pimpinellifolium* LA1589 (**a**) or Yellow Pear (**b**) leaves treated with 100 nM flg22 or flgII-28 peptides derived from the flagellin sequence of *Pst* DC3000 (DC3000) or *Pcal* ES4326 (ES4326) and measured in relative light units (RLUs). Results shown are means and s.d. (n = 8 plants). **c,** Bacterial populations of *Pst* (cfu/cm^2) were measured from LA1589 and Yellow Pear plants. Plants were first infiltrated with 10^8 cfu/mL of heat-killed *Pst* DC3000Δ*avrPto*Δ*avrPtoB*Δ*hopQ1-1*Δ*fliC* (*Pst* DC3000ΔΔΔΔ) complemented with different *fliC* alleles (ES4326 or DC3000) or no *fliC* (empty vector)[12], and 16 hours later were inoculated with *Pst* DC3000ΔΔΔΔ at 5 x 10^4 cfu/mL. Bacterial populations were measured 2 days after bacterial inoculation. Results shown are the individual values from each plant and s.d. (n = 4). **d,** Bacterial populations of *Pcal* ES4326 (cfu/cm^2) were measured from F2 plants segregating for *FLS3* and *fls3-1*. Plants were infiltrated with *Pst* DC3000ΔΔΔΔ complemented with ES4326 *fliC* followed by *Pcal* ES4326 and bacterial populations were measured as described in (**c**). Results shown are the individual values from each plant and s.d. (LA1589, n = 6; *FLS3/FLS3*, n = 9; *FLS3/fls3-1*, n

= 11; *fls3-1/fls3-1*, $n = 7$; Yellow Pear, $n = 6$). **e,** Representative plants inoculated as described in (**d**) except *Pcal* ES4326 was inoculated at 1 x 10^5 cfu/mL. Photos were taken 4 days after bacterial inoculation. For all experiments, different letters indicate significant differences using Tukey-Kramer HSD test ($P < 0.05$) and similar results were obtained in three independent experiments.

Figure 3. *FLS3* confers flgII-28 sensitivity. a, Immunodetection of phosphorylated MAPKs in Yellow Pear protoplasts expressing either FLS3 or EFR and treated with 100 nM flg22, flgII-28 or elf18. Immunoblot analysis using anti-phospho-p44/42 (α-P-ERK, top panel) detects phosphorylated MAPKs while anti-HA (lower panel) demonstrates the presence of FLS3-HA or EFR-HA. Asterisk indicates non-specific labeling. Similar results were obtained in two independent experiments. **b, c, d,** Oxidative burst produced by *N. benthamiana* leaves expressing either FLS3, FLS3 variants, or YFP treated with 100 nM flgII-28 or water, and measured in relative light units (RLU). Results shown are means ± s.d. ($n = 4$ plants), and all constructs were expressed in the same leaves. Similar results were obtained in three independent experiments.

Figure 4. FLS3 directly and specifically binds flgII-28. a, Structures of probes flgII-28* and flg22*. The probes including a bifunctional photo-crosslinking moiety attached to the N-termini of flgII-28 and flg22, which includes a diazirine photolabile functionality and the alkyne handle for click chemistry. **b,** Photo-affinity labeling of FLS3-GFP demonstrates direct and specific binding to flgII-28. Immunoblot analysis using streptavidin-HRP (top panel) demonstrates the presence of biotin-labeled FLS3-flgII-28 or FLS2-flg22 complexes, while re-analysis of the blot with anti-GFP antibodies (bottom panel) shows the presence of FLS3-GFP or FLS2-GFP in the samples. **c, d**, Binding assays using flgII-28* or flg22* peptides show the concentration dependence of the receptor-ligand interactions. Immunoblot analysis using streptavidin-HRP (top

panel) shows biotin-labeled FLS3-flgII-28 (**c**) or FLS2-flg22 (**d**) complexes, and re-analysis of the blot with anti-GFP antibodies (bottom panel) shows the presence of FLS3-GFP or FLS2-GFP in all samples. The split blots for (**c**) are results from different experiments. **e, f,** Competitive binding assays using 25 nM flgII-28* and excess unmodified flgII-28 (**e**) or flg22 (**f**) peptides. Immunoblot analysis using streptavidin-HRP (top panel) shows biotin-labeled FLS3-flgII-28 complexes, and re-analysis of the blot with anti-GFP antibodies (bottom panel) shows the presence of FLS3-GFP in all samples. For all parts, similar results were obtained in at least two independent experiments.

Figure 5. FLS3 signaling is BAK1-dependent and is suppressed by effectors. a, Oxidative burst produced by *N. benthamiana* leaves silenced for *BAK1* or a control gene by VIGS, expressing *FLS3* and treated with 100 nM flgII-28 or elf18, and measured in relative light units (RLU). Results shown are means ± s.d. (n = 4 plants). **b,** FLS3 can be found in a complex with BAK1 specifically after treatment with flgII-28. *N. benthamiana* leaves expressing either FLS3-GFP or FLS2-GFP in combination with AtBAK1-Myc, and treated with buffer alone, 1 μM flgII-28, or 1 μM flg22 for 2 minutes before harvesting, were used for immunoprecipitation using anti-GFP affinity resin. BAK1-Myc is pulled down with both FLS3-GFP and FLS2-GFP after treatment with flgII-28 or flg22, respectively, but not buffer alone (top panel) though both samples contain BAK1-Myc (middle panel), and FLS3-GFP or FLS2-GFP is also present (bottom panels). **c, d,** Oxidative burst produced by *N. benthamiana* leaves expressing FLS3 in combination with either YFP, AvrPto, or AvrPtoB$_{1\text{-}387}$ and treated with 100 nM flgII-28, and measured in relative light units (RLU). For each experiment, the construct combinations were expressed in the same leaves. Results are means ± s.d. (n = 4 plants). For all parts, similar results were obtained in three independent experiments.

Methods

Plant materials and growth conditions. Seeds of *S. lycopersicum* 'Yellow Pear', *S. pimpinellifolium* accession LA1589, F1 hybrids, and F2s were provided by Esther van der Knapp. Seeds of *S. lycopersicum* 'Heinz1706' were provided by James Giovannoni. Other accessions of *S. pimpinellifolium* were obtained from the Tomato Genetics Resource Center (http://tgrc.ucdavis.edu/). Seeds of *S. lycopersicum* cv. 'Matt's Wild Cherry' and 'Galapagos' used for generating the F2 segregating populations were obtained from Good Mind Seeds (http://goodmindseeds.org/). Tomato and *N. benthamiana* plants were grown as previously described[6,41].

Materials. The sequences of flg22 (Biomatik), T1 version of flgII-28 (EZBiolab; Biomatik), DC3000 version of flgII-28 (Genscript), ES4326 version of flgII-28 (Genscript), and elf18 (Biomatik) have been described previously[11,42,43]. The T1 version of flgII-28 was used for all experiments except where otherwise indicated. For generation of flg22 probe, flg22 peptide with lysine 13 protected by Fmoc was used (Biomatik). 2-[4-({Bis[(1-tert-butyl-1H-1,2,3-triazol-4 yl)methyl]amino}methyl)-1H-1,2,3-triazol-1-yl] acetic acid (BTTAA) and 2-[2-(Prop-2-ynyloxy)ethoxy]-4-[3-(trifluoromethyl)-3H-diazirin-3yl]benzoic acid were prepared as described previously[44,45]. Low resolution mass spectrometry was performed on an HPLC-MS system equipped with a diode array detector and connected to a Quattro II spectrometer (Micromass/Waters) operated in positive electrospray ionization (ESI^+) mode. Data acquisition and processing for the HPLC-MS was controlled by Waters Masslynx software. For semi-preparative HPLC, a Phenomenex Jupiter Proteo C-12 column (25 cm x 10 mm, 4 µm particle diameter) was used.

506 **Oxidative burst bioassay**. The production of ROS was detected using a luminol-based assay as
507 previously described[12]. Measurements were taken every 2 minutes for 32 minutes, and the
508 average ROS production for each plant was the mean of 3-4 leaf disks. Total ROS production
509 was determined by summing the average RLU values for the time points between 0 and 32
510 minutes after treatment.
511 **DNA libraries.** DNA libraries were generated according to Zhong[46] with the following
512 modifications. Genomic DNA was isolated using DNeasy Plant Mini Kit (Qiagen) and equal
513 amounts of gDNA were pooled into 3 samples that included 15, 14, and 15 plants each. For each
514 sample, 500 ng of DNA was fragmented using NEBNext dsDNA Fragmentase (New England
515 Biolabs) for 40 minutes at room temperature before stopping the reaction with EDTA at a final
516 concentration of 125 mM. Fragmented gDNA enriched for fragments around 250 to 500 bp were
517 purified using AMPure XP beads and eluted in water. End-repair, dA-tailing, Y-shape adaptor
518 ligation, triple-SPRI purification and size selection, and PCR enrichment was performed as
519 described[46]. The uniquely barcoded libraries from the three samples were mixed for a final
520 concentration of 5 ng/µL and 50 ng of library was sent to the Genomics Resources Core facility
521 at Weill Cornell Medical College (New York, NY) for sequencing on 1 lane of an Illumina
522 HiSeq 2500. The read length was 51 bp and average insert size was 200 bp. Sequences were
523 submitted to the NCBI project number PRJNA263381 and data from this study can be accessed
524 through the Solgenomics ftpsite (ftp://ftp.solgenomics.net/). Sequences from the two parental
525 accessions were obtained from a previous study[47].
526 **Sequence assembly.** Reads were inspected for quality using FastQC
527 (http://www.bioinformatics.babraham.ac.uk/projects/fastqc/) and cleaning was performed with
528 fastq-mcf (https://code.google.com/p/ea-utils/wiki/FastqMcf). A reference Yellow Pear genome

was previously generated[47]. F2 reads were mapped to the Yellow Pear genome using bowtie2([48]) and reads with a mapping quality less than 20 were removed. SNPs were called with Samtools[49] and LA1589-specific SNPs were identified as follows: homozygous SNPs were found by selecting SNP positions with at least 30x coverage in each parental accessions and discarding any sites with a SNP in Yellow Pear. LA1589-specific SNP frequency was calculated using Varscan[50] at F2 sites with a read coverage greater than 15 base pairs and plotted with loess fitting using R[51]. The effect of each SNP and indel in the parental genomes was determined previously[47]. Sequence data are available as accession PRJNA263381 at NCBI (http://www.ncbi.nlm.nih.gov/bioproject/263381).

Phylogenetic analysis. A phylogenetic analysis was performed using tomato genotyping data[14] from 75 cultivars and *S. pimpinellifolium* accessions. Two alignments were generated by concatenating the SNP sites, one using whole genome data and another using data from 1-10 Mb on chromosome 4. Two unrooted maximum likelihood trees were generated with Mega v. 5.2([52]) using a GTR substitution model and gamma-rate distribution among sites. Nearest-Neighbor-Interchange was used as the heuristic tree search method with 100 bootstrap samples. For homolog analysis, *FLS3* from *Solanum lycopersicum* 'Heinz1706'([53]) was aligned with Muscle to its closest homologs from *Solanum tuberosum*[54], *Solanum melongena*[55], *Capsicum annuum*[56], *Nicotiana benthamiana*[57], *Petunia inflata* and *Arabidopsis thaliana* as determined from BLAST. A rooted Maximum Likelihood tree was generated as described above using the *Arabidopsis thaliana* homolog as an outgroup. Orthology to *FLS3* was determined by reciprocal BLAST and synteny analysis.

Virulence assays in tomato

Pseudomonas cannabina pv. *alisalensis* ES4326 (formerly *P. syringae* pv. *maculicola*[12]) and *Pseudomonas syringae* pv. *tomato* DC3000Δ*avrPto*Δ*avrPtoB*Δ*hopQ1-1*Δ*fliC* strains were grown on King's B solid media, and bacterial suspensions were prepared in 10 mM $MgCl_2$ and 0.02% Silwet L-77. Plants were vacuum-infiltrated as previously described[58]. The PTI induction assays used *Pst* DC3000Δ*avrPto*Δ*avrPtoB*Δ*hopQ1-1*Δ*fliC* strains that were transformed with constructs that allowed for expression of *fliC* variants from either *Pst* DC3000 or *Pcal* ES4326[12]. Bacterial suspensions of 10^8 cfu/mL were boiled for 5 minutes to kill the bacteria, and the resulting solutions were used for vacuum infiltration to induce PTI. After 16 hours, plants were vacuum infiltrated with either *Pst* DC3000Δ*avrPto*Δ*avrPtoB*Δ*hopQ1-1*Δ*fliC* or *Pcal* ES4326 at 5 x 10^4 or 1 x 10^5 cfu/mL. Inoculated plants were kept in a growth chamber until sampled to determine bacterial populations two or three days after infiltration, or to take photographs four days after infiltration.

Primer design and PCR conditions. Primers were designed using the Primer3 program[59]. DNA was genotyped from 28 flgII-28 insensitive individuals used in the original DNA library generation. PCR products were amplified using standard cycling conditions. PCR products and restriction enzyme digested DNA were separated by agarose gel electrophoresis.

Cloning. *FLS3* was amplified from cDNA using KOD Hot Start DNA polymerase (Merck Millipore) and gene-specific primers (5'-CACCATGCTTAGTAACATCATGGAGAAACA-3' and 5'-ATTTACTTCTATGTTTCCAAATGTGTTCT-3'), then cloned into the Gateway entry vector pENTR/D-TOPO (Life Technologies). *EFR* was amplified from *Arabidopsis thaliana* Col-0 cDNA using gene-specific primers (5'-ATGAAGCTGTCCTTTTCACTTG-3' and 5'-ACATAGTATGCATGTCCGTATTTAAC-3') and cloned into pJLSmart as previously described[58]. *FLS2* was amplified from *FLS2p::SlFLS2-GFP* in pCAMBIA2300([60]) using gene-

574 specific primers (5’- CACCATGATGATGTTAAAGACAGTTG-3’ and 5’-
575 ATCTTTTACCAAATGAGAAGG-3’), then cloned into pENTR/D-TOPO. Gateway
576 recombination reactions using LR Clonase II was performed according to the manufacturer’s
577 recommendations (Life Technologies). Destination vectors pGWB417 (C-terminal 4xMyc
578 fusion) and pGWB505 (C-terminal sGFP fusion)[61] were used for transient expression in *N.*
579 *benthamiana*, and destination vector HBT95 (C-terminal 2xHA fusion)[62] was used for transient
580 expression in tomato protoplasts. Genomic sequences of *FLS3* were amplified from tomato
581 cultivars and *S. pimpinellifolium* accessions using Gateway compatible primers (5’-
582 GGGGACAAGTTTGTACAAAAAAGCAGGCTTCTGATCAAGGGAAGTGGACAGA-3’
583 and 5’-
584 GGGGACCACTTTGTACAAGAAAGCTGGGTTACCTCTTCAACTATTCAAACTACG-3’)
585 and were recombined into pDONR221 via recombination reactions using BP Clonase according
586 to the manufacturer’s recommendations (Life Technologies). Amino acid substitutions were
587 introduced with Pfu Turbo polymerase PCR reactions using the Stratagene QuikChange
588 mutagenesis protocol with the following primer pairs (nucleotide changes underlined):
589 K877Q, 5’-CTAGTGGAATTGTGGTTGCAATTCAGGTACTGGATTTG-3’ and 5’-
590 CAAATCCAGTACCTGAATTGCAACCACAATTCCACTAG-3’;
591 T1011P, 5’-GGCACATACAAAGACATTAGGCCCTCTTGGATATATTGC-3’ and 5’-
592 GCAATATATCCAAGAGGGCCTAATGTCTTTGTATGTGCC-3’;
593 P1011T, 5’-GGCACATACAAAGACATTAGGCACTCTTGGATATATTGC-3’ and 5’-
594 GCAATATATCCAAGAGTGCCTAATGTCTTTGTATGTGCC-3’.
595 **Protoplast transfection and MAPK assays**. Protoplast isolation and transfection was
596 performed based on previously described methods[63] with the following modifications. Leaf strips

were digested overnight in the dark in enzyme solution consisting of 1X MS salts (Sigma-Aldrich), 1X MS vitamins (Sigma-Aldrich), 12% sucrose, 0.4% cellulose (Yakult) and 0.015% macerozyme (Yakult). Protoplasts were released and passed through a 100 μm mesh filter. Protoplast solution was layered with W5 solution and centrifuged for 4 minutes at 400 x g with acceleration and brakes off. The interface layer containing intact protoplasts was removed, washed and resuspended in W5 solution, and incubated on ice for 1.5 to 2 hours with frequent mixing. Intact protoplasts were resuspended in MMg solution and counted, and 8 x 10^4 protoplasts in 200 μL volume were mixed with 10 μg of plasmid DNA for transfection using PEG solution. Transfection was stopped after 10 minutes, and protoplasts were recovered WI solution for 6 hours in the dark.

For the MAPK assays protoplasts were treated with peptides (flg22, flgII-28, or elf18) diluted in WI buffer for a final concentration 100 nM. Samples were incubated for 15 minutes before protoplasts were harvested and flash-frozen in liquid nitrogen. Total proteins were solubilized using 3X Laemmli sample buffer and immunoblotting was performed as described below. In order to detect phosphorylated (i.e. active) MAPK proteins, an anti-phospho-p44/42 MAPK T202/Y204 antibody (Cell Signaling; 9101) was used for immunoblotting.

Virus-induced gene silencing (VIGS) and *Agrobacterium*-mediated transient expression.

VIGS was performed as previously described[64] using gene fragments for control-VIGS (*EC1*)[6] and *BAK1*-VIGS[64]. For transient gene expression, leaves of 4- to 6-week old *N. benthamiana* plants were infiltrated with *Agrobacterium* bacterial suspensions prepared as described[58] with slight modifications. Bacteria were suspended in induction media[65] and incubated at room temperature with shaking for 5-6 hours before preparing bacterial infiltration suspension. Plants were kept for 24 hours before collecting samples for ROS analysis, or for 48 hours before

collecting samples for immunoblot analysis. All constructs were infiltrated at a final OD_{600} of 0.1-0.2, and were mixed at equal concentrations with a construct expressing the viral suppressor of silencing *p19* except for those used to infiltrate VIGS plants.

Quantitative reverse transcriptase PCR (qRT-PCR). Total RNA was isolated from *N. benthamiana* leaves using the Plant RNeasy Mini Kit (Qiagen). RNA was treated with TURBO DNA-free kit (Life Technologies) twice for 30 minutes at 37°C with 1.0 U DNase for each treatment. One µg of RNA was used to prepare cDNA using RevertAid First Strand cDNA Synthesis Kit (Thermo Scientific). Quantitative RT-PCR was performed with sequence specific primers and cycling conditions as described previously[66] on ABI Prism 7900 HT Sequence Detection System (Applied Biosystems) with iTaq Universal SYBR Green Supermix (Bio-Rad). Data were normalized using *NbUbq*[66].

Co-immunoprecipitation. Total protein was extracted from *Agrobacterium*-infiltrated *N. benthamaiana* leaf tissue at 1mg/mL in extraction buffer consisting of 50 mM Tris-HCl pH 7.5, 150 mM NaCl, 0.5% Triton X-100, 1% (v/v) plant protease inhibitor cocktail (Sigma-Aldrich), 1 mM Na_3VO_4, 1 mM NaF, and 20 mM β-glycerophosphate (modified from Koller and Bent[67]). After clearing by centrifugation, soluble proteins were incubated with EZview Red Anti-c-Myc affinity gel (Sigma-Aldrich) or GFP-Trap_A slurry (ChromoTek GmbH) for 1 hour at 4°C. Resin was washed three times with cold extraction buffer, and one time with cold 50 mM Tris-HCl pH 7.5 before eluting with 2X Laemmli sample buffer. For input samples, 5-15 µL soluble protein was mixed with 2X sample buffer.

Immunoblotting. To confirm protein expression in *N. benthamiana* plants, total protein was extracted in extraction buffer consisting of 50 mM Tris-HCl, pH 7.5, 10% glycerol, 2 mM EDTA, 5 mM DTT, 1% Triton X-100, 1% (v/v) plant protease inhibitor cocktail (Sigma-

643 Aldrich), and 6 µg protein was resolved by SDS-PAGE before transfer to PVDF membrane
644 (Merck Millipore). Proteins were detected with anti-phospho-p44/42 MAPK T202/Y204 (Cell
645 Signaling; 9101), anti-HA-HRP conjugate (Roche; 12013819001), anti-Myc-HRP conjugate
646 (Santa Cruz; sc-789), streptavidin-HRP conjugate (Invitrogen; S-911), anti-GFP (Roche;
647 118144660001), or anti-AvrPto[68], with secondary antibodies anti-rabbit IgG-HRP conjugate
648 (Promega; W4011) or anti-mouse IgG-HRP conjugate (Santa Cruz; sc-2005) when necessary,
649 followed by chemiluminescent visualization. Ponceau S solution (Sigma-Aldrich) staining was
650 used to verify equal loading.
651 **Generation of peptide probes.** The N-hydroxysuccinimide activated ester of the benzoic acid
652 probe was added in dimethyl sulfoxide (63.5 mM) to a solution of MAMP peptide in PBS buffer,
653 pH 8.0 (1:6 H_2O/DMSO) and allowed to react for 2 hours. The solution was then dried by
654 lyophilization and the resulting MAMP peptide probe was either purified by semi-preparative
655 HPLC or for flg22 the lyophilized powder was dissolved in 20% piperidine (Sigma-Aldrich) in
656 dimethylformamide (Fisher Scientific) and allowed to react for 3 hours for Fmoc deprotection,
657 then purified by semi-preparative HPLC.
658 **Plasma membrane enrichment, binding and photo-crosslinking with MAMP probes, and**
659 **biotinylation using click chemistry**. Membrane protein enrichment was performed according to
660 Broghammer[69] with the following modifications. Frozen *N. benthamiana* leaves were
661 homogenized in extraction buffer (30 g fresh weight tissue in 200 mL buffer) consisting of 50
662 mM MOPS-KOH, pH 7.5, 500 mM D-sorbitol, 5 mM DTT, 5 mM EDTA, 1%
663 polyvinylpyrrolidone (PVP), and 1 mM phenylmethylsulfonyl fluoride (PMSF). After miracloth
664 filtration and initial centrifugation, the homogenate was centrifuged at 100,000 x g for 75
665 minutes at 4°C. The resulting microsomal pellet was suspended in 25 mM Tris-HCl, pH 7.5, 250

mM sucrose, 10 mM potassium phosphate, pH 7.5, and 28.8 mM NaCl. Using aqueous two-phase partitioning, plasma membrane-enriched microsomes were purified using a bulk phase with 6% Dextran Mr 450,000-650,000 (Sigma-Aldrich) and 6% polyethylene glycol 3350 (Sigma-Aldrich).The upper phase was centrifuged at 100,000 x g for 2 hours at 4°C, and the plasma membrane-enriched microsome pellet was suspended in 2 mL cold binding buffer consisting of 25 mM MES, pH 6.0, 3 mM $MgCl_2$, and 10 mM NaCl, and the sample was equally divided before the addition of peptides. Plasma membrane-enriched microsomes were incubated with peptides for 15 minutes in the dark at 4°C to allow for binding to occur before irradiating for 15 minutes using a UV lamp (Blak-Ray B-100AP 100-watt lamp, UVP Ultraviolet Products) at a working distance of 2.5 cm. The plasma membrane-enriched microsomes were solubilized in binding buffer containing 1% Triton X-100 and 0.1% SDS (v/v). GFP-tagged receptors were immunoprecipitated overnight at 4°C using 10 µl of GFP-Trap_A slurry per sample (ChromoTek GmbH). The resin was washed twice with 1X PBS pH7.4 and twice with radioactivity immune precipitation assay (RIPA) buffer consisting of 1X PBS pH 7.4, 1% Triton X-100, 0.5% sodium deoxycholate and 0.1% SDS. Next, the resin was suspended in click chemistry buffer consisting of RIPA buffer, 500 µM BTTAA, 250 µM $CuSO_4$ pentahydrate, 2 mM sodium ascorbate and 100 µM azide-PEG4-biotin conjugate (Click Chemistry Tools) in a total volume of 250 µL and placed on a rotatory shaker at 4°C for 2-6 hours. The resin was washed as described above before the immunoprecipitated material was eluted by boiling for 5 minutes in 3X Laemmli sample buffer.

688 **References**

689 41. Velasquez, A.C., Chakravarthy, S. & Martin, G.B. Virus-induced gene silencing (VIGS) in
690 *Nicotiana benthamiana* and tomato. ***J. Visualiz. Exper.*** **28**,
691 http://www.jove.com/index/Details.stp?ID=1292 (2009).

692 42. Felix, G., Duran, J.D., Volko, S. & Boller, T. Plants have a sensitive perception system for
693 the most conserved domain of bacterial flagellin. *Plant J* **18**, 265-76 (1999).

694 43. Kunze, G. ***et al.*** The N terminus of bacterial elongation factor Tu elicits innate immunity in
695 *Arabidopsis* plants. *Plant Cell* **16**, 3496-507 (2004).

696 44. Besanceney-Webler, C. ***et al.*** Increasing the efficacy of bioorthogonal click reactions for
697 bioconjugation: a comparative study. *Angew Chem Int Ed Engl* **50**, 8051-6 (2011).

698 45. Mayer, T. & Maier, M.E. Design and synthesis of a tag-free chemical probe for
699 Photoaffinity Labeling. ***Eur. J. Org. Chem.***, 4711-4720 (2007).

700 46. Zhong, S. ***et al.*** High-throughput illumina strand-specific RNA sequencing library
701 preparation. *Cold Spring Harb Protoc*, 940-9 (2011).

702 47. Strickler, S. ***et al.*** Comparative genomics and phylogenetic discordance of cultivated tomato
703 and close wild relatives. *PeerJ* **3:e793** (2015).

704 48. Langmead, B. & Salzberg, S.L. Fast gapped-read alignment with Bowtie 2. *Nature Methods*
705 **9**, 357-U54 (2012).

706 49. Li, H. ***et al.*** The Sequence Alignment/Map format and SAMtools. *Bioinformatics* **25**, 2078-
707 2079 (2009).

708 50. Koboldt, D.C. ***et al.*** VarScan 2: somatic mutation and copy number alteration discovery in
709 cancer by exome sequencing. *Genome Res* **22**, 568-76 (2012).

710 51. Team, R.C. R: A Language and Environment for Statistical Computing. (R Foundation for
711 Statistical Computing, Vienna, Austria, 2014).

712 52. Tamura, K. ***et al.*** MEGA5: molecular evolutionary genetics analysis using maximum
713 likelihood, evolutionary distance, and maximum parsimony methods. *Mol Biol Evol* **28**,
714 2731-9 (2011).

715 53. Tomato Genome, C. The tomato genome sequence provides insights into fleshy fruit
716 evolution. *Nature* **485**, 635-41 (2012).

717 54. Potato Genome Sequencing, C. *et al.* Genome sequence and analysis of the tuber crop
718 potato. *Nature* **475**, 189-95 (2011).

719 55. Hirakawa, H. *et al.* Draft genome sequence of eggplant (*Solanum melongena* L.): the
720 representative Solanum species indigenous to the old world. *DNA Res* (2014).

721 56. Kim, S. *et al.* Genome sequence of the hot pepper provides insights into the evolution of
722 pungency in *Capsicum* species. *Nat Genet* **46**, 270-8 (2014).

723 57. Bombarely, A. *et al.* A draft genome sequence of *Nicotiana benthamiana* to enhance
724 molecular plant-microbe biology research. *Mol Plant Microbe Interact* **25**, 1523-30 (2012).

725 58. Mathieu, J., Schwizer, S. & Martin, G.B. Pto kinase binds two domains of AvrPtoB and its
726 proximity to the effector E3 ligase determines if it evades degradation and activates plant
727 immunity. *PLoS Pathog* **10**, e1004227 (2014).

728 59. Untergasser, A. *et al.* Primer3Plus, an enhanced web interface to Primer3. *Nucleic Acids Res*
729 **35**, W71-4 (2007).

730 60. Robatzek, S. *et al.* Molecular identification and characterization of the tomato flagellin
731 receptor LeFLS2, an orthologue of *Arabidopsis* FLS2 exhibiting characteristically different
732 perception specificities. *Plant Mol Biol* **64**, 539-47 (2007).

733 61. Nakagawa, T. *et al.* Improved Gateway binary vectors: high-performance vectors for
734 creation of fusion constructs in transgenic analysis of plants. *Biosci Biotechnol Biochem* **71**,
735 2095-100 (2007).

736 62. He, P. *et al.* Specific bacterial suppressors of MAMP signaling upstream of MAPKKK in
737 *Arabidopsis* innate immunity. *Cell* **125**, 563-575 (2006).

738 63. He, P., Shan, L. & Sheen, J. The use of protoplasts to study innate immune responses. *Plant-*
739 *Pathogen Interactions* **354**, 1-10 (2006).

740 64. Chakravarthy, S., Velasquez, A.C., Ekengren, S.K., Collmer, A. & Martin, G.B.
741 Identification of *Nicotiana benthamiana* genes involved in pathogen-associated molecular
742 pattern-triggered immunity. *Mol Plant-Microbe Interact* **23**, 715-26 (2010).

743 65. Sessa, G., D'Ascenzo, M. & Martin, G.B. Thr38 and Ser198 are Pto autophosphorylation
744 sites required for the AvrPto-Pto-mediated hypersensitive response. *EMBO J* **19**, 2257-69
745 (2000).

746 66. Mantelin, S. *et al.* The receptor-like kinase SlSERK1 is required for Mi-1-mediated
747 resistance to potato aphids in tomato. *Plant J* **67**, 459-71 (2011).

67. Koller, T. & Bent, A.F. FLS2-BAK1 extracellular domain interaction sites required for defense signaling activation. *PLoS One* **9**, e111185 (2014).

68. Shan, L., He, P., Zhou, J.M. & Tang, X. A cluster of mutations disrupt the avirulence but not the virulence function of AvrPto. *Mol Plant-Microbe Interact* **13**, 592-8 (2000).

69. Broghammer, A. *et al.* Legume receptors perceive the rhizobial lipochitin oligosaccharide signal molecules by direct binding. *Proc Natl Acad Sci U S A* **109**, 13859-64 (2012).

70. Robatzek, S. & Wirthmueller, L. Mapping FLS2 function to structure: LRRs, kinase and its working bits. *Protoplasma* **250**, 671-81 (2013).

71. Pruitt, R.N. *et al.* The rice immune receptor XA21 recognizes a tyrosine-sulfated protein from a Gram-negative bacterium. *Science Advances* **1**(2015).

Extended Data Table 1. Sequence, restriction enzyme and expected product size of genotyping primers. Underlined bold letters are mismatched bases used in dCAPS primers. Expected PCR product size, or product size of CAPS and dCAPS primers after digestion using the restriction enzymes indicated**.**

Extended Data Table 2. List of *fls3* mutant alleles, positions of indels and SNPs, and the number of amino acids in the predicted protein size. The tomato cultivars and *S. pimpinellifolium* accessions listed were found to have the indicated *fls3* alleles. Numbers in parentheses indicate the nucleotide position(s) using the *S. lycopersicum* 'Heinz1706' coding sequence as reference. Nucleotide changes were considered SNPs if they differed from either Heinz1706 or *S. pimpinellifolium* accession LA1589 sequences.

Extended Data Figure 1. Identification of additional flgII-28 insensitive tomato cultivars and confirmation of genotyping results using additional F2 populations. a, b, c, Oxidative

burst produced by tomato or *S. pimpinellifolium* leaves treated with 100 nM of either flg22 or flgII-28 and measured in relative light units (RLU). Results shown are means ± s.d. (n = 4 plants per cultivar). Similar results were obtained in at least two independent experiments. **d**, Oxidative burst produced by tomato leaves treated with 1 μM of either flg22 or flgII-28 and measured in relative light units (RLU). Results shown are the means ± s.d. (n = 3 plants with one disk each for Rio Grande, Matt's Wild Cherry and Galapagos; n = 4 disks from 1 plant each for F1 plants). **e,** Phenotyping results as measured by oxidative burst after 1 μM flgII-28 treatment of leaf disks from plants derived from each of three populations. Numbers indicate the number of F2 plants that showed either increased reactive oxygen species production (sensitive) or no oxidative burst (insensitive) after flgII-28 treatment; all plants were tested in parallel with flg22. Chi-squared tests supported a segregation ratio of 3:1 (sensitive:insensitive) in two of the three populations. **f,** Genotyping results of *FLS3* in Rio Grande x Matt's Wild Cherry and Rio Grande x Galapagos F2 populations. Numbers indicate the number of F2 plants with the Rio Grande allele of *FLS3* for each phenotype. **g,** Transcript abundance measured as RPKM (reads per kilobase of exon model per million mapped reads) of *FLS3* (*Solyc04g009640*) and *FLS2.1* (*Solyc02g070890*) 6 hours after syringe-infiltration into leaves of 1 μM flg22 or flgII-28, or vacuum-infiltration of the bacterial strains *Pst* DC3000 or DC3000Δ*avrPto*Δ*avrPtoB* (Δ*avrPto*Δ*avrPtoB*) at 5 x 10^6 cfu/mL (see Rosli *et al*.[5] for further details). Results shown are the means ± 95% confidence interval (n = 3 experiments except for flg22 treatment where n = 2 and its corresponding mock inoculation where n = 4). Different letters indicate significant differences using Tukey-Kramer HSD test ($P < 0.05$).

Extended Data Figure 2. Whole-genome mapping results for *FLS3*. The frequency of LA1589-specific SNPs was plotted according to genome location along each Yellow Pear

chromosome. By mapping F2 reads to the Yellow Pear genome assembly, a coverage depth of 12X was obtained and reads covered 94% of the Yellow Pear genome after mapping quality filtering and duplicate read removal. By plotting LA1589-specific SNP frequency across the Yellow Pear chromosomes, a 2.9 Mb region (from 2.619 to 5.486 Mb) on chromosome 4 was identified as being linked to flgII-28 sensitivity, indicated by the arrow.

Extended Data Figure 3. Maximum likelihood trees generated from tomato SNP data for selected accessions using whole-genome SNPs. a, SNPs[14] from each chromosome or **b,** from chromosome 4 found between 1 and 10 Mb were concatenated. Trees are unrooted and the number of supporting bootstrap values for 100 replications is shown. All cultivars are *S. lycopersicum* except the LA accessions which are *S. pimpinellifolium*. Boxes indicate cultivars that have a close relationship on Chromosome 4 (**b**) including known flgII-28 insensitive cultivars which are indicated with asterisks.

Extended Data Figure 4. FLS3 functional domains and phylogenetic analysis. a, Amino acid changes found in *fls3* alleles are bold and underlined, and details provided in grey boxes. The K877Q amino acid substitution which is expected to interfere with kinase activity[19] is indicated. The kinase catalytic site shows that FLS3 is a non-RD kinase as it has the residues CD[18]. Dots serve as placeholders to facilitate demonstration of the conserved residues in the aligned LRR repeats. Modeled after Robatzek[70]. **b,** Phylogenetic analysis of *FLS3* and homologs from Solanaceous species. Branches are annotated with bootstrap support (100 replicates). Gene identifiers correspond to the following species: *Solanum lycopersicum* 'Heinz1706' (Tomato) - *Solyc04g012110.1.1*, *Solyc04g012100.1.1*, *Solyc04g009640.2.1*; *Solanum tuberosum* (Potato) - *PGSC0003DMC400040896_PGSC0003DMT400060766*, *PGSC0003DMC400040897_PGSC0003DMT400060777*,

820 *PGSC0003DMC400028022_PGSC0003DMT400041350*; *Solanum melongena* (Eggplant) -
821 *Sme2.5_04364.1_g00001.1*; *Capsicum annum* (Pepper) - *CA05g03880*; *Nicotiana benthamiana*
822 (Wild tobacco) – *Niben101Scf06774g02012.1*/*Niben101Scf06774g02013.1*; *Petunia axillaris*
823 (Petunia) - *Peaxi162Scf00569g03016.1*; *Arabidopsis thaliana* (Arabidopsis) – *AT5G46330.1*.
824 The homolog in *N. benthamiana* is predicted as two gene models, but is likely a mis-annotation.
825 The box indicates *FLS3* and its predicted orthologs. **c,** Oxidative burst produced by *Petunia*
826 *axillaris* leaves treated with 100 nM flg22 or flgII-28 and measured in relative light units (RLU).
827 Results shown are means ± s.d. (n = 4 plants). **d,** Summary of response to flg22 or flgII-28
828 treatment in all plant species tested. (+) indicates sensitivity to peptide treatment while (–)
829 indicates insensitivity.
830 **Extended Data Figure 5. *FLS3* is associated with enhanced resistance to bacterial infection.**
831 **a,** Bacterial populations of *Pcal* ES4326 (cfu/cm^2) were measured from F2 plants segregating for
832 *FLS3* or *fls3-1*. Plants were infiltrated with bacterial suspensions of 3 x 10^4 cfu/mL and bacterial
833 populations were measured 3 days after infiltration. Results shown are the individual values from
834 each plant and s.d. (LA1589, n = 6; *FLS3/FLS3*, n = 8; *FLS3/fls3-1*, n = 15; *fls3-1/fls3-1*, n = 6;
835 Yellow Pear, n = 6). Different letters indicate significant differences using Tukey-Kramer HSD
836 test ($P < 0.05$) and similar but not always statistically significant results were obtained in five
837 independent experiments. **b,** Representative plants infiltrated as described in (**a**) except *Pcal*
838 ES4326 was inoculated at 1 x 10^5 cfu/mL, and photos were taken 4 days after bacterial
839 infiltration. **c,** Representative plants infiltrated as described in Fig. 2c except *Pst*
840 DC3000Δ*avrPto*Δ*avrPtoB*Δ*hopQ1-1*Δ*fliC* (DC3000ΔΔΔΔ) was inoculated at 1 x 10^5 cfu/mL.
841 Photos of LA1589 and Yellow Pear plants were taken 4 or 3 days after bacterial infiltration,
842 respectively. **d,** Bacterial populations of *Pcal* ES4326 (cfu/cm^2) were measured from F2 plants

segregating for *FLS3* or *fls3-1*. Plants were first infiltrated with bacterial suspensions of 10^8 cfu/mL of heat-killed *Pst* DC3000ΔΔΔΔ complemented with DC3000 *fliC*, and 16 hours later were inoculated with bacterial suspensions of *Pcal* ES4326 at 5 x 10^4 cfu/mL. Bacterial populations were measured 2 days after bacterial infiltration. Results shown are the individual values from each plant and s.d. (LA1589, $n = 6$; *FLS3/FLS3*, $n = 6$; *FLS3/fls3-1*, $n = 16$; *fls3-1/fls3-1*, $n = 7$; Yellow Pear, $n = 9$). Different letters indicate significant differences using Tukey-Kramer HSD test ($P < 0.05$); however, no consistent differences were observed between three independent experiments. **e,** Representative plants infiltrated as described in (**d**) except *Pcal* ES4326 was inoculated at 1 x 10^5 cfu/mL, and photos were taken 4 days after bacterial infiltration.

Extended Data Figure 6. Immunoblot analysis of *Agrobacterium*-mediated transient protein expression in *N. benthamiana* leaves. Except where indicated otherwise, each immunoblot depicts four plant samples per construct or construct combination from one experiment. Untransformed (-) controls are included to show non-specific antibody labeling. **a**, Protein levels of FLS3-Myc corresponding to Figure 3b. Top panel: immunoblotting with anti-Myc antibodies. Bottom panel: Ponceau S staining to demonstrate equal loading. **b**, Protein levels of FLS3-Myc and FLS3 kinase domain mutants FLS3(K877Q)-Myc and FLS3(T1011P)-Myc corresponding to Figure 3c. Top panel: immunoblotting with anti-Myc antibodies. Bottom panel: Ponceau S staining to demonstrate equal loading. **c**, Protein levels of FLS3-Myc, FLS3-2-Myc and FLS3-2(P1011T)-Myc corresponding to Figure 3d. Top panel: immunoblotting with anti-Myc antibodies. Bottom panel: Ponceau S staining to demonstrate equal loading. **d**, Protein levels of FLS3-Myc corresponding to Figure 5a. Top panel: immunoblotting with anti-Myc antibodies. Bottom panel: Ponceau S staining to demonstrate equal loading. **e**, Protein levels of FLS3-Myc,

YFP-Myc and AvrPto-Myc corresponding to Figure 5c. From top panel (1) to bottom panel (4). Panel 1: immunoblotting with anti-Myc antibodies. Panel 2: immunoblotting with anti-GFP antibodies. Panel 3: immunoblotting with anti-AvrPto antibodies. Panel 4: Ponceau S staining to demonstrate equal loading. **f**, Protein levels of FLS3-Myc, YFP-Myc and AvrPtoB$_{1-387}$-Myc corresponding to Figure 5d. From top panel (1) to bottom panel (3). Panel 1: immunoblotting with anti-Myc antibodies. Panel 2: immunoblotting with anti-GFP antibodies. Panel 3: Ponceau S staining to demonstrate equal loading. Asterisk indicates non-specific labeling.

Extended Data Figure 7. Peptide affinities and experimental scheme for binding experiments. a-d, EC50 predictive modeling curves used to estimate EC50 values in (**e**). Oxidative burst produced by Rio Grande tomato leaves treated with concentrations of flgII-28 and flg22 peptides or probes ranging from 1 to 1000 nM and measured in relative light units (RLU). Data points shown are individual total ROS production for each concentration (n = 4 plants). The fitted curves were predicted by the JMP software using the non-linear logistic 4p formula as described previously[71] with predicted EC50 value indicated by the vertical dashed line. Similar results were obtained in four independent experiments. **e,** Estimated EC50 for flgII-28 and flg22 peptides or probes using values obtained in four independent experiments as described above. Data points shown are the inferred EC50 values and s.d. (n = 4). **f,** Experimental scheme for binding experiments. Plasma membrane-enriched microsomes were harvested from *N. benthamiana* leaf tissue expressing FLS3-GFP (or FLS2-GFP), incubated with indicated concentrations of either peptide-probes (flgII-28* or flg22*) or peptide-probes with unmodified competitor peptides (flgII-28 or flg22) followed by UV-irradiation at 365 nm. Immunoprecipitated FLS3-GFP was used in a "click" reaction with biotin azide and analyzed by immunoblotting.

Extended Data Figure 8. FLS3 signaling requires BAK1 and FLS3 associates with BAK1 *in vivo* in a flgII-28-dependent manner. a, Relative expression of different *SERK* genes in *N. benthamiana* leaves silenced for *BAK1* or a control gene by VIGS was determined using quantitative real-time reverse transcription PCR (qRT-PCR) with primers described previously[66]. The relative expression of the *SERK* genes was normalized using *NbUbq*. Results shown are the means ± s.d. (n = 4 plants per construct). Similar results were obtained in two independent experiments; however, while the *SERK3* transcript was significantly different in both experiments, the reduction of *SERK2* transcript was not significantly reduced in the second experiment. Different letters indicate significant differences using Student's t-test ($P < 0.05$). **b**, Oxidative burst produced by *N. benthamiana* leaves silenced for *BAK1* by VIGS, expressing *FLS3* in combination with either *YFP* or At*Bak1* and treated with 100 nM flgII-28, and measured in relative light units (RLU). Both construct combinations were expressed in the same leaves. Results shown are means ± s.d. (n = 4 plants per experiment). **c,** FLS3 can be found in a complex with BAK1 specifically after treatment with flgII-28. *N. benthamiana* leaves expressing either FLS3-GFP or FLS2-GFP in combination with AtBAK1-Myc, and treated with buffer alone, 1 μM flgII-28, or 1 μM flg22 for 2 minutes before harvesting, were used for immunprecipitation using anti-c-Myc affinity resin. Both FLS3 and FLS2 are pulled down with BAK1 after treatment with 1 μM flgII-28 or flg22, respectively, but not buffer alone (top panel) though both samples contain FLS3-GFP or FLS2-GFP (middle panel), and BAK1-Myc is also present (bottom panels). Similar results were obtained in three independent experiments. **d,** FLS3 can specifically associate with BAK1. *N. benthamiana* leaves expressing FLS3-GFP in combination with either AtBAK1-Myc or YFP-Myc, and treated for 10 minutes with 1 μM flgII-28 before harvesting, were used for immunprecipitation using anti-c-Myc affinity resin. FLS3 is pulled

912 down with BAK1 but not with YFP (top panel) though both samples contain FLS3-GFP (middle
913 panel), and immunoprecipitated BAK1-Myc and YFP-Myc are also present (bottom panel). For
914 parts **b-d**, similar results were obtained in three independent experiments.
915
916

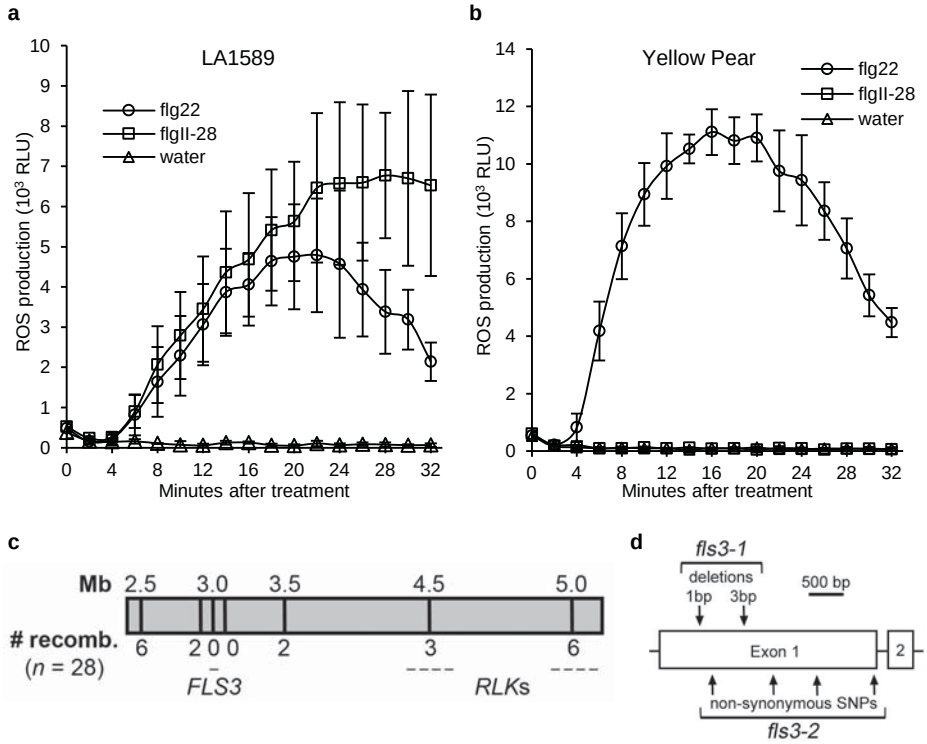

Figure 1. flgII-28 responsiveness is associated with a region on Chromosome 4 in tomato. a, b, Oxidative burst produced by *S. pimpinellifolium* LA1589 (**a**) or *S. lycopersicum* cv. 'Yellow Pear' (**b**) leaves treated with 100 nM flg22 or flgII-28, or with water, and measured in relative light units (RLU). Results shown are means ± s.d. (n = 4 plants). Similar results were obtained in three independent experiments. **c,** Fine mapping of the chromosome 4 region associated with flgII-28 sensitivity. Marker positions are indicated by the vertical black bars, and the number of plants showing recombination (# recomb.) is indicated. The approximate locations of 9 LRR-RLK genes are indicated by horizontal bars. **d,** Mutant allele deletions and SNPs are indicated on the gene model of *FLS3* (*Solyc04g009640*).

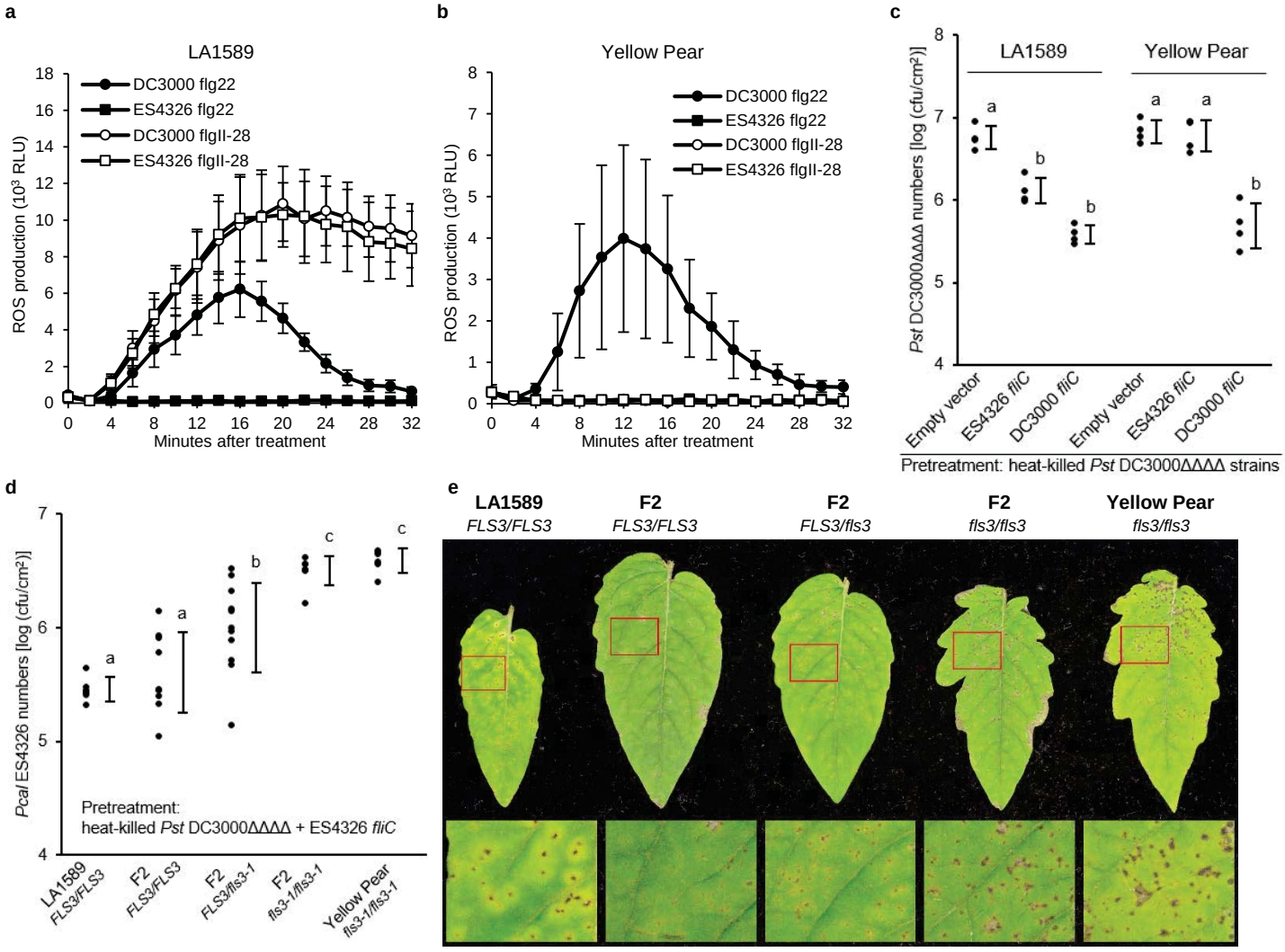

Figure 2. FLS3 is associated with enhanced resistance to bacterial infection. a, b, Oxidative burst produced by *S. pimpinellifolium* LA1589 (**a**) or Yellow Pear (**b**) leaves treated with 100 nM flg22 or flgII-28 peptides derived from the flagellin sequence of *Pst* DC3000 (DC3000) or *Pcal* ES4326 (ES4326) and measured in relative light units (RLUs). Results shown are means and s.d. (n = 8 plants). **c**, Bacterial populations of *Pst* (cfu/cm^2) were measured from LA1589 and Yellow Pear plants. Plants were first infiltrated with 10^8 cfu/mL of heat-killed *Pst* DC3000Δ*avrPto*Δ*avrPtoB*Δ*hopQ1-1*Δ*fliC* (DC3000ΔΔΔΔ) complemented with different *fliC* alleles (ES4326 or DC3000) or no *fliC* (empty vector)[12], and 16 hours later were inoculated with *Pst* DC3000ΔΔΔΔ at 5 x 10^4 cfu/mL. Bacterial populations were measured 2 days after bacterial inoculation. Results shown are the individual values from each plant and s.d. (n = 4). **d,** Bacterial populations of *Pcal* ES4326 (cfu/cm^2) were measured from F2 plants segregating for *FLS3* and

fls3-1. Plants were infiltrated with *Pst* DC3000ΔΔΔΔ complemented with ES4326 *fliC* followed by *Pcal* ES4326 and bacterial populations were measured as described in (**c**). Results shown are the individual values from each plant and s.d. (LA1589, $n = 6$; *FLS3/FLS3*, $n = 9$; *FLS3/fls3-1*, $n = 11$; *fls3-1/fls3-1*, $n = 7$; Yellow Pear, $n = 6$). **e,** Representative plants inoculated as described in (**d**) except *Pcal* ES4326 was inoculated at 1 x 10^5 cfu/mL. Photos were taken 4 days after bacterial inoculation. For all experiments, different letters indicate significant differences using Tukey-Kramer HSD test ($P < 0.05$) and similar results were obtained in three independent experiments.

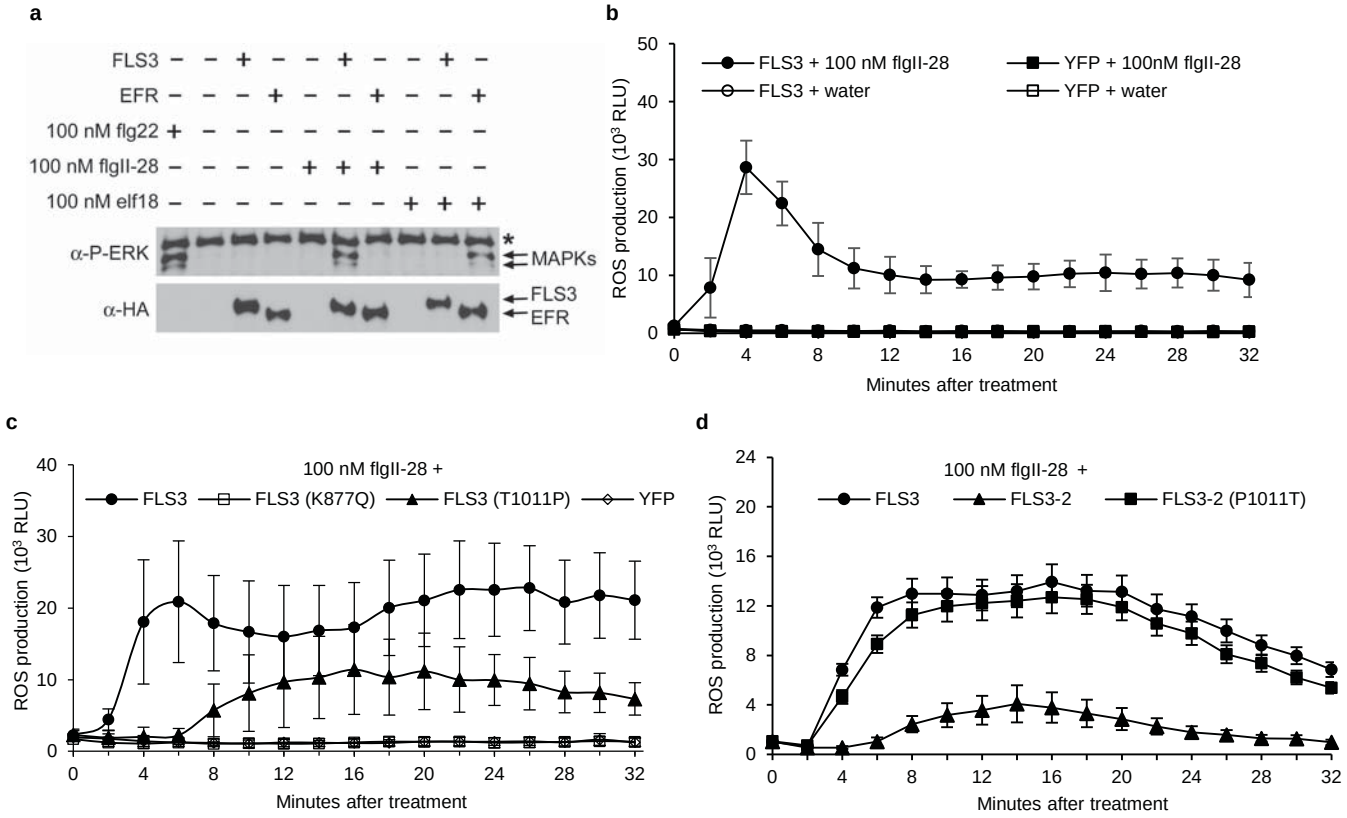

Figure 3. ***FLS3*** **confers flgII-28 sensitivity. a,** Immunodetection of phosphorylated MAPKs in Yellow Pear protoplasts expressing either FLS3 or EFR and treated with 100 nM flg22, flgII-28 or elf18. Immunoblot analysis using anti-phospho-p44/42 (α-P-ERK, top panel) detects phosphorylated MAPKs while anti-HA (lower panel) demonstrates the presence of FLS3-HA or EFR-HA. Asterisk indicates non-specific labeling. Similar results were obtained in two independent experiments. **b, c, d,** Oxidative burst produced by *N. benthamiana* leaves expressing either FLS3, FLS3 variants, or YFP treated with 100 nM flgII-28 or water (**b**), or 100 nM flgII-28 alone (**c, d**) and measured in relative light units (RLU). Results shown are means ± s.d. (n = 4 plants), and all constructs were expressed in the same leaves. Similar results were obtained in three independent experiments.

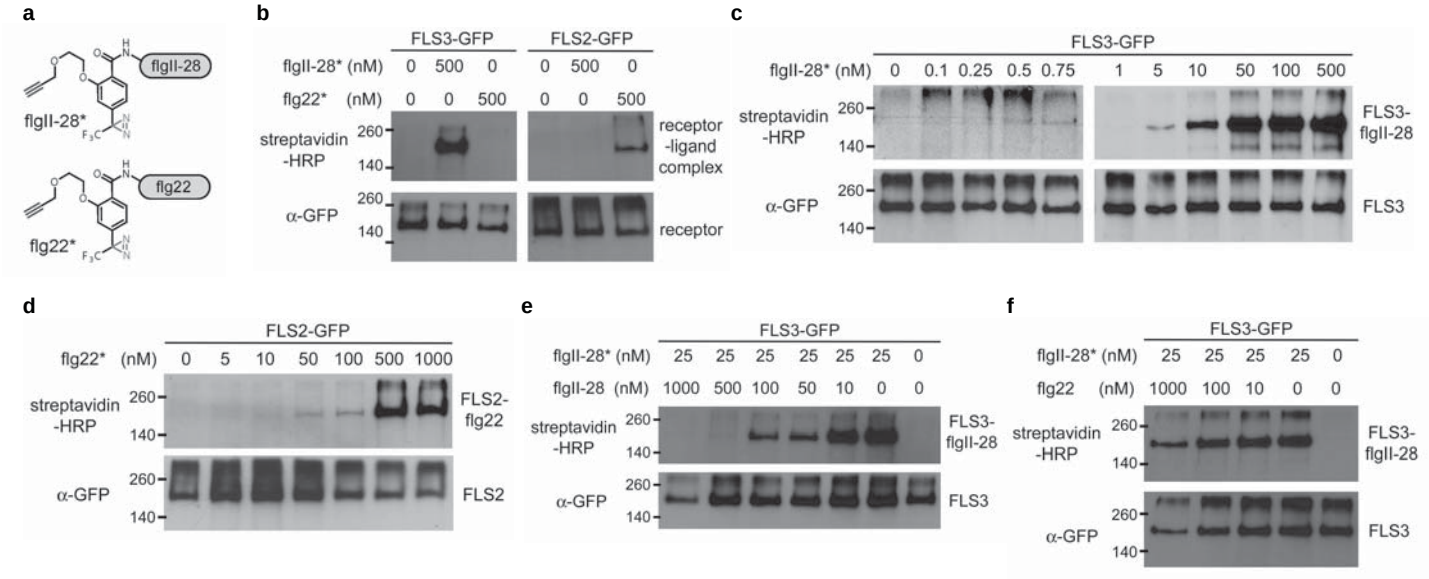

Figure 4. FLS3 directly and specifically binds flgII-28. a, Structures of probes flgII-28* and flg22*. The probes including a bifunctional photo-crosslinking moiety attached to the N-termini of flgII-28 and flg22, which includes a diazirine photolabile functionality and the alkyne handle for click chemistry. **b,** Photo-affinity labeling of FLS3-GFP demonstrates direct and specific binding to flgII-28*. Immunoblot analysis using streptavidin-HRP (top panel) demonstrates the presence of biotin-labeled FLS3-flgII-28* or FLS2-flg22* complexes, while re-analysis of the blot with anti-GFP antibodies (bottom panel) shows the presence of FLS3-GFP or FLS2-GFP in the samples. **c, d**, Binding assays using flgII-28* or flg22* peptides show the concentration dependence of the receptor-ligand interactions. Immunoblot analysis using streptavidin-HRP (top panel) shows biotin-labeled FLS3-flgII-28* (**c**) or FLS2-flg22* (**d**) complexes, and re-analysis of the blot with anti-GFP antibodies (bottom panel) shows the presence of FLS3-GFP (**c**) or FLS2-GFP (**d**) in all samples. The split blots for (**c**) are results from different experiments. **e, f,** Competitive binding assays using 25 nM flgII-28* and excess unmodified flgII-28 (**e**) or flg22 (**f**) peptides. Immunoblot analysis using streptavidin-HRP (top panel) shows biotin-labeled FLS3-flgII-28* complexes, and re-analysis of the blot with anti-GFP antibodies (bottom panel) shows the presence of FLS3-GFP in all samples. For all parts, similar results were obtained in at least two independent experiments.

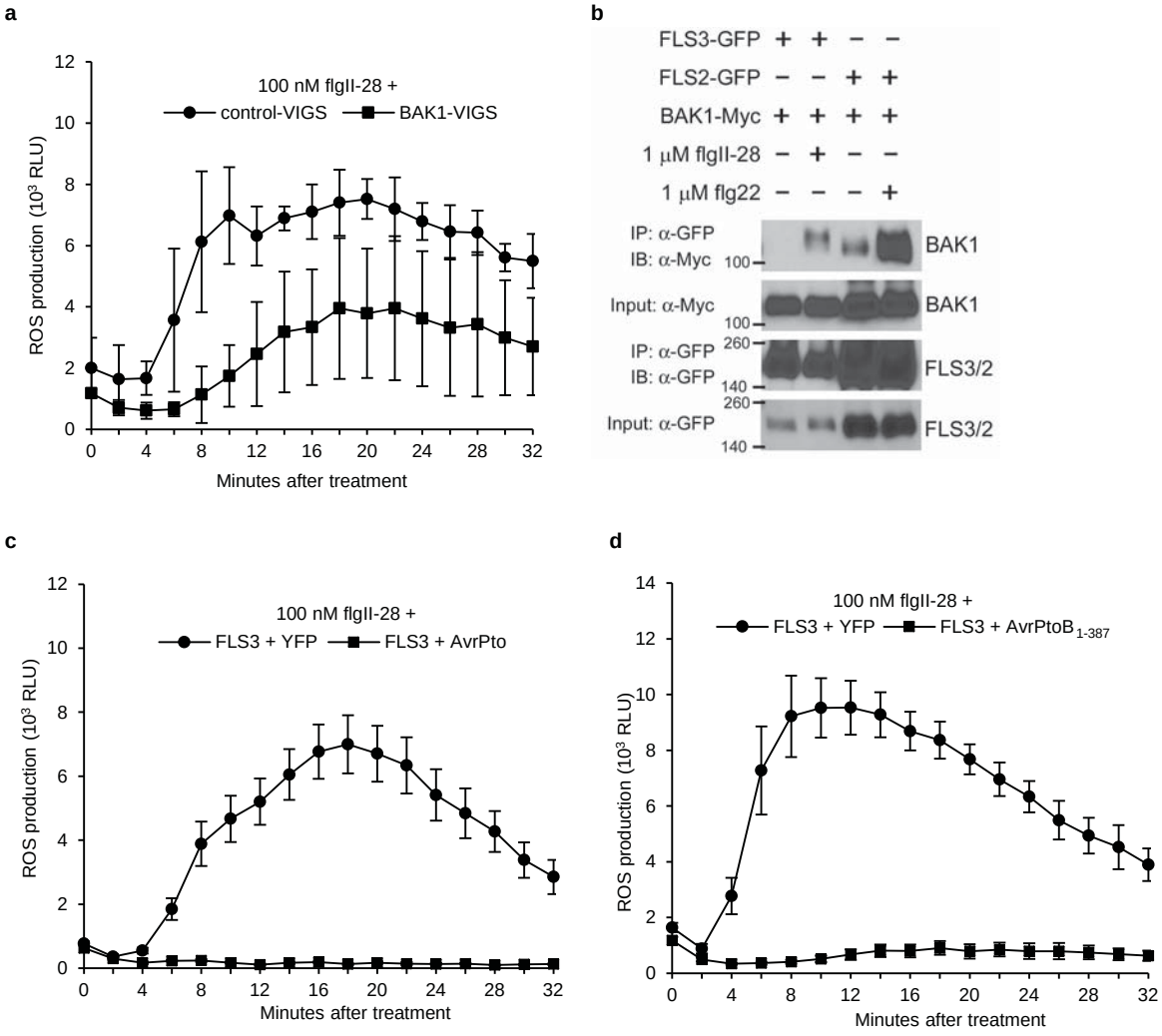

Figure 5. FLS3 signaling is BAK1-dependent and is suppressed by effectors. a, Oxidative burst produced by *N. benthamiana* leaves silenced for *BAK1* or a control gene by VIGS, expressing FLS3 and treated with 100 nM flgII-28, and measured in relative light units (RLU). Results shown are means ± s.d. (n = 4 plants). **b,** FLS3 can be found in a complex with BAK1 specifically after treatment with flgII-28. *N. benthamiana* leaves expressing either FLS3-GFP or FLS2-GFP in combination with AtBAK1-Myc, and treated with buffer alone, 1 μM flgII-28, or 1 μM flg22 for 2 minutes before harvesting, were used for immunoprecipitation using anti-GFP affinity resin. BAK1-Myc is pulled down with both FLS3-GFP and FLS2-GFP after treatment with flgII-28 or flg22, respectively, but not buffer alone (top panel) though both samples contain BAK1-Myc (middle panel), and FLS3-GFP or FLS2-GFP is also present (bottom panels). **c, d,** Oxidative burst produced by *N. benthamiana* leaves expressing FLS3 in

combination with either YFP, AvrPto, or AvrPtoB$_{1-387}$ and treated with 100 nM flgII-28, and measured in relative light units (RLU). For each experiment, the construct combinations were expressed in the same leaves. Results are means ± s.d. (n = 4 plants). For all parts, similar results were obtained in three independent experiments.

Extended Data Table 1.

Primer name	Ch. 4 region (Mb)	5' primer	3' primer	Restriction enzyme	YP allele (bp)	LA1589 allele (bp)
Solcap_snp_64142	2.4135	TCCATTTGAAAAAGATTTGTTTTTTG**A**GCT	TCCTCGGCTCCACAATCTTA	SacI	212	182, 30
Solcap_snp_21372	2.9158	TGATTGTGGATTAAGGAATTTTGGT**A**	CAATCACCGGACTCCATAGC	RsaI	131	106,25
Ch04_3.0997	3.0997	TGGAACCCGATTTTTCATGT	GGGATCAACAAAGGGGATTT	BfaI	284,132	416
Ch04_3.1105_YP	3.1105	CACGTAATTCACAATATTAAGCAGTT	TTGCAAAAATTTCCCTCAAGA	-	268	-
Ch04_3.1105_1589	3.1105	CACGTAATTCACAATATTAAGCAGTC	GCTGGGTTCAAGTTGATGGT	-	-	194
Solcap_snp_25082	3.5042	TGACGTAACACCTGTTGGAA	GGACCATCAGCACAAGTTTC	EcoRV	287,148	435
Solcap_snp_51721	4.4392	TCTTGGTGATGGGATTTGGT	TGAACTTGGCAACATCAAAAA	XhoI	507	379,128
Solcap_snp_41575	4.9426	CAACACCGTACATTTTCCCAA	ACAGGGGACAGAAACGTCAT	RsaI	312	267, 45
BAV1971	3.0153	AAGAAGATTCGGAATTCTACCTGA	CGGTGGTGAAATGTGGAACG	-	-	756

Extended Data Table 1. Sequence, restriction enzyme and expected product size of genotyping primers. Underlined bold letters are mismatched bases used in dCAPS primers. Expected PCR product size, or product size of CAPS and dCAPS primers after digestion using the restriction enzymes indicated.

Extended Data Table 2.

Tomato cultivars and *S. pimpinellifolium* accessions	Allele designation	Insertion	Deletions	SNPs	Protein length (aa)
Yellow Pear 'Galapagos tomato' Gold Ball Livingston Matt's Wild Cherry Pepper Tomato Red Pear San Marzano Yellow Plum LA1279	*fls3-1*	1 bp (3053)	1 bp (551) 3 bp (1213-1215)	G to A (791) G to A (1641) G to A (1919)	184
LA0373	*fls3-2*			T to A (57) A to G (657) G to A (661) A to G (1585) G to T (2145) A to C (3031)	1135

Extended Data Table 2. List of fls3 mutant alleles, positions of indels and SNPs, and the number of amino acids in the predicted protein size. The tomato cultivars and *S. pimpinellifolium* accessions listed were found to have the indicated *fls3* alleles. Numbers in parentheses indicate the nucleotide position(s) using the *S. lycopersicum* 'Heinz1706' coding sequence as reference. Nucleotide changes were considered SNPs if they differed from either Heinz1706 or *S. pimpinellifolium* accession LA1589 sequences.

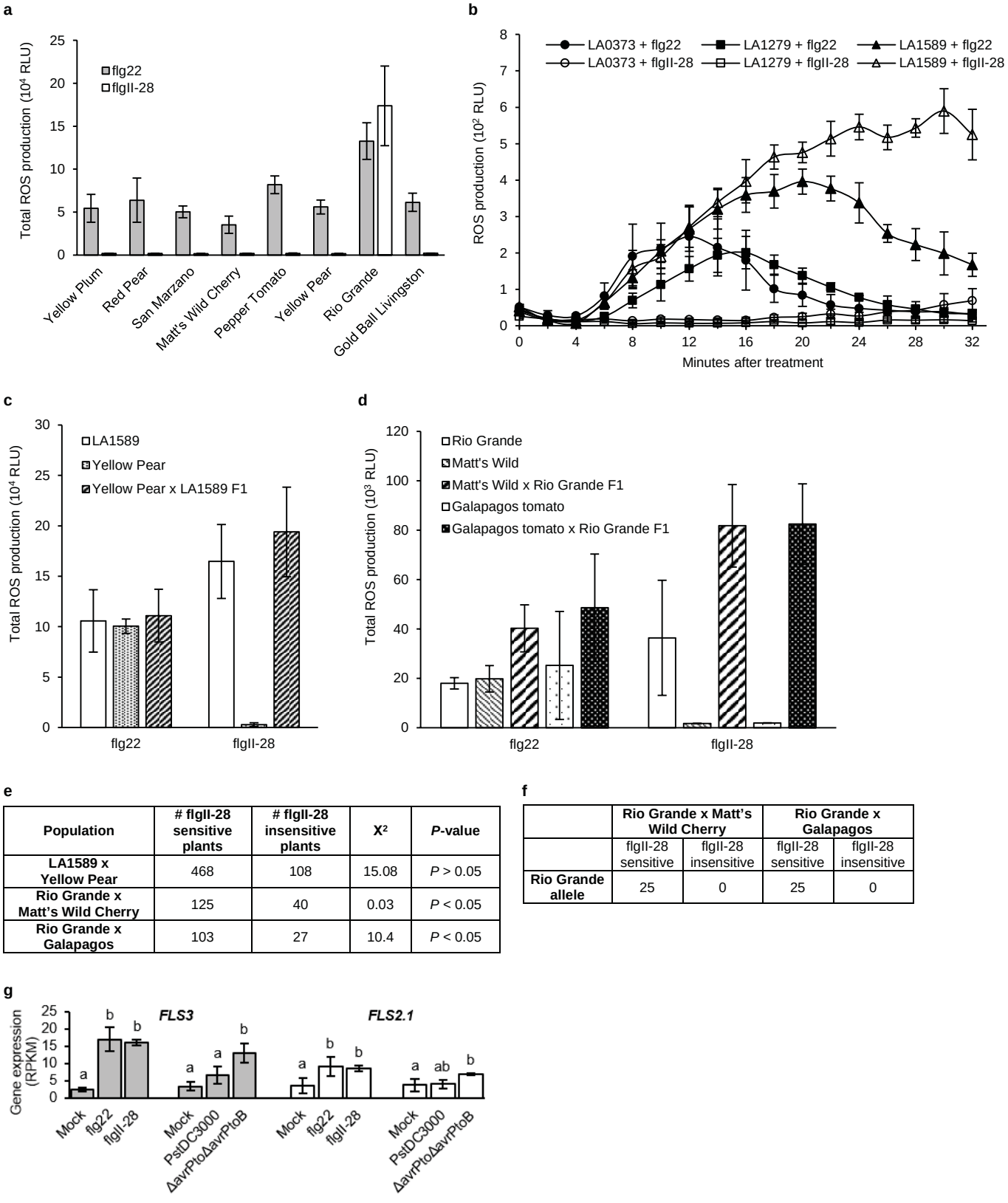

e

Population	# flgII-28 sensitive plants	# flgII-28 insensitive plants	X^2	*P*-value
LA1589 x Yellow Pear	468	108	15.08	$P > 0.05$
Rio Grande x Matt's Wild Cherry	125	40	0.03	$P < 0.05$
Rio Grande x Galapagos	103	27	10.4	$P < 0.05$

f

	Rio Grande x Matt's Wild Cherry		Rio Grande x Galapagos	
	flgII-28 sensitive	flgII-28 insensitive	flgII-28 sensitive	flgII-28 insensitive
Rio Grande allele	25	0	25	0

Extended Data Figure 1. Identification of additional flgII-28 insensitive tomato cultivars and confirmation of genotyping results using additional F2 populations. a,b,c, Oxidative burst produced by tomato or *S. pimpinellifolium* leaves treated with 100 nM of either flg22 or flgII-28 and measured in

relative light units (RLU). Results shown are means ± s.d. (n = 4 plants per cultivar). Similar results were obtained in at least two independent experiments. **d,** Oxidative burst produced by tomato leaves treated with 1 μM of either flg22 or flgII-28 and measured in relative light units (RLU). Results shown are the means ± s.d. (n = 3 plants with one disk each for Rio Grande, Matt's Wild Cherry and Galapagos; n = 4 disks from 1 plant each for F1 plants). **e,** Phenotyping results as measured by oxidative burst after 1μM flgII-28 treatment of leaf disks from plants derived from each of three populations. Numbers indicate the number of F2 plants that showed either increased reactive oxygen species production (sensitive) or no oxidative burst (insensitive) after flgII-28 treatment; all plants were tested in parallel with flg22. Chi-squared tests supported a segregation ratio of 3:1 (sensitive:insensitive) in two of the three populations. **f,** Genotyping results of *FLS3* in Rio Grande x Matt's Wild Cherry and Rio Grande x Galapagos F2 populations. Numbers indicate the number of F2 plants with the Rio Grande allele of *FLS3* for each phenotype. **g,** Transcript abundance measured as RPKM (reads per kilobase of exon model per million mapped reads) of *FLS3* (*Solyc04g009640*) and *FLS2.1* (*Solyc02g070890*) 6 hours after syringe-infiltration into leaves of 1 μM flg22 or flgII-28, or vacuum-infiltration of the bacterial strains *Pst* DC3000 or DC3000Δ*avrPto*Δ*avrPtoB* (Δ*avrPto*Δ*avrPtoB*) at 5 x 10^6 cfu/mL (see Rosli et al.[5] for further details). Results shown are the means ± 95% confidence interval (n = 3 experiments except for flg22 treatment where n = 2 and its corresponding mock inoculation where n = 4). Different letters indicate significant differences using Tukey-Kramer HSD test ($P < 0.05$).

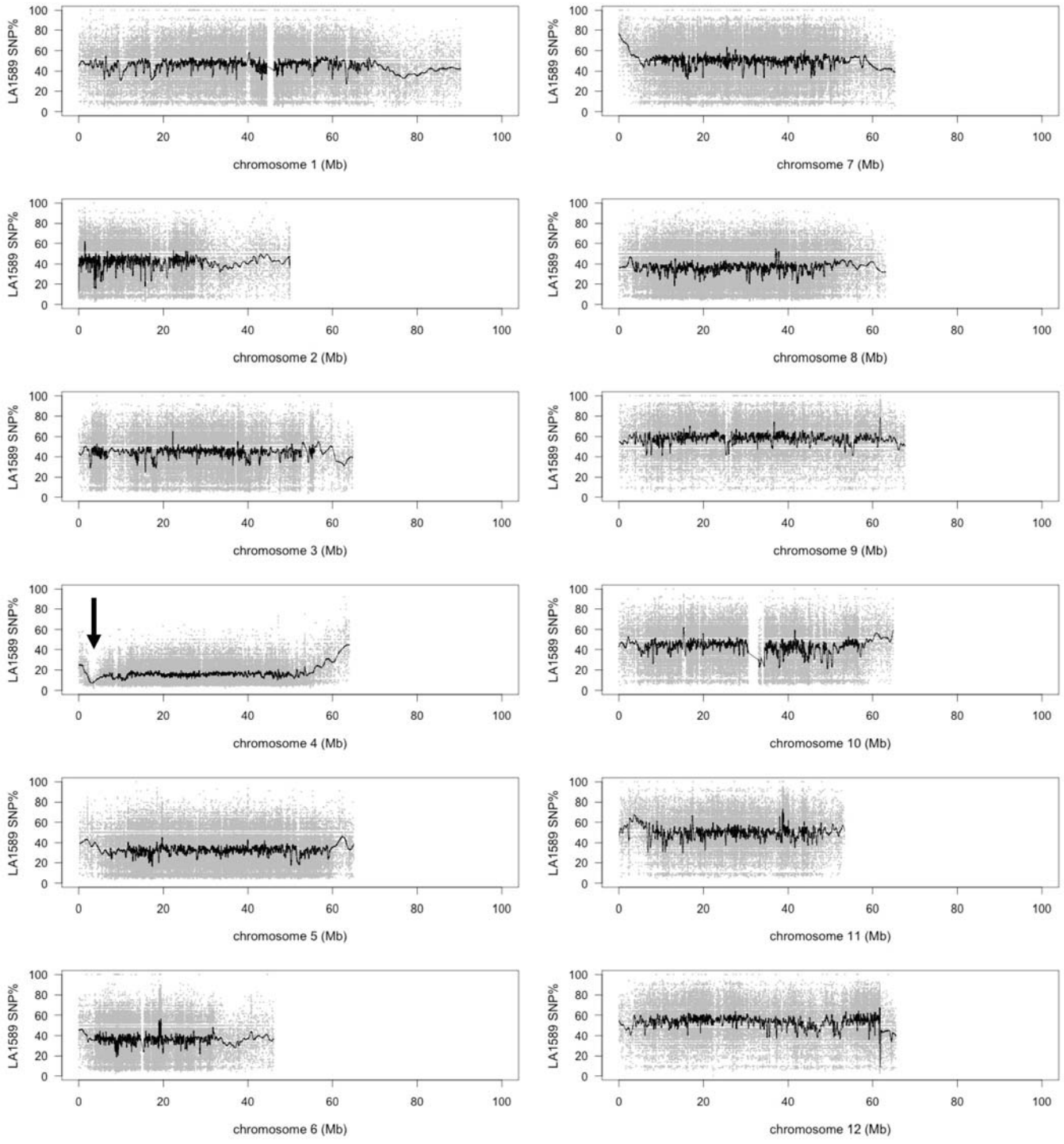

Extended Data Figure 2. Whole-genome mapping results for *FLS3*. The frequency of LA1589-specific SNPs was plotted according to genome location along each Yellow Pear chromosome. By mapping F2 reads to the Yellow Pear genome assembly, a coverage depth of 12X was obtained and reads covered 94% of the Yellow Pear genome after mapping quality filtering and duplicate read removal. By plotting LA1589-specific SNP frequency across the Yellow Pear chromosomes, a 2.9 Mb region (from 2.619 to 5.486 Mb) on chromosome 4 was identified as being linked to flgII-28 sensitivity, indicated by the arrow.


a
Brandywine(Sudduth/Quisenberry)
Cherokee Purple
Orange Strawberry
Tomatedellugar
Gold Ball
Burbank
Rosso Monserrat
PARAGON
Beauty
Favorite
Globe
Medford
Black From Tula
Oxheart
Amish Paste
Cotaxtla I
Opalka
Howard German
Oregon Spring
Severianin
Pearson
Aker's West Virginia
Marglobe
Legend
Siletz
Heinz 1706
Piedmont
Summit
Cherokee
Heinz 1370
Oregon Star
E6203
Rio Grande
M82
Sponzillo
Tainan
Moneymaker
Devon Surprise
Juane Flammee
Hong Kong
Grushovka
King Humbert
Black Plum
Stupice
Principe Borghese
Yellow Stuffer
LYC1903
Alisa Craig
San Marzano*
Roma VF
Rutgers
White Queen
Prospero
Pomodoro Superselezionedi Marmande
Costoluto Genovese
Turrialba
Ponderosa
Rinon PI98097
Tomate
Sao Paulo
Yellow Pear*
Rumi Banjan
D'Olivia x Industria
Peron
Purple Calabash
Rinon PI118783
LA2135
LA2078
LA2077
LA2076
LA2137
Marveille des Marches
LA2131
Large German Cherry
VFNT Cherry
b
Pomodoro Superselezione di Marmande
Costoluto Genovese
King Humbert
Principe Borghese
Devon Surprise
Moneymaker
Yellow Stuffer
Stupice
Black Plum
Juane Flammee
Globe
Cherokee
Orange Strawberry
D'Olivia x Industria
White Queen
Hong Kong
Rutgers
LA2135
Prospero
Rinon PI118783
LYC1903
Grushovka
Oxheart
Black From Tula
LA2077
Sao Paulo
Tomate
LA2078
Ponderosa
Turrialba
LA2076
LA2131
LA2137
VFNT Cherry
Marveille des Marches
Large German Cherry
Sponzillo
Tainan
Tomatedellugar
Peron
Alisa Craig
Siletz
Amish Paste
Yellow Pear*
Rumi Banjan
Purple Calabash
Gold Ball
San Marzano*
Summit
Piedmont
Opalka
Howard German
Medford
Legend
Cherokee Purple
Brandywine (Sudduth/Quisenberry)
Roma VF
PARAGON
Heinz 1370
Beauty
Favorite
Rosso Monserrat
Burbank
Rinon PI98097
M82
E6203
Aker's West Virginia
Marglobe
Pearson
Rio Grande
Heinz 1706
Cotaxtla I
Severianin
Oregon Star
Oregon Spring

Extended Data Figure 3. Maximum likelihood trees generated from tomato SNP data for selected accessions using whole-genome SNPs. **a,** SNPs[14] from each chromosome or **b,** from chromosome 4 found between 1 and 10 Mb were concatenated. Trees are unrooted and the number of supporting bootstrap values for 100 replications is shown. All cultivars are *S. lycopersicum* except the LA accessions which are *S. pimpinellifolium*. Boxes indicate cultivars that have a close relationship on Chromosome 4 (**b**) including known flgII-28 insensitive cultivars which are indicated with asterisks.

a

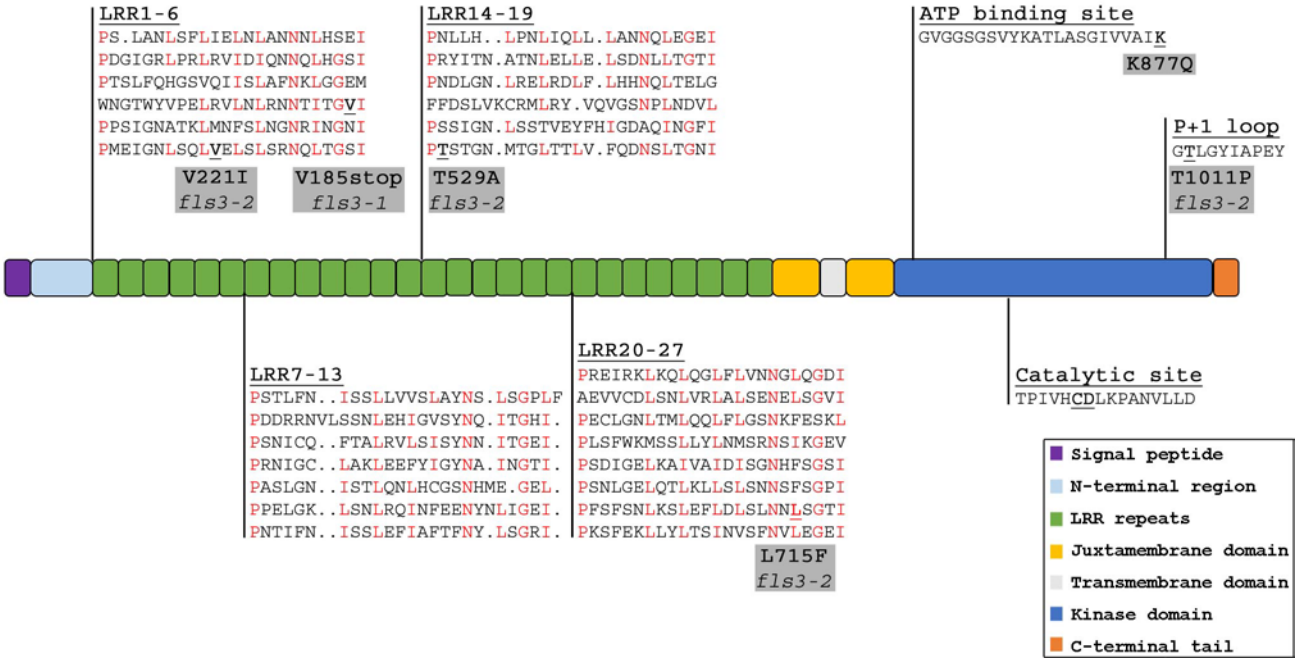

b

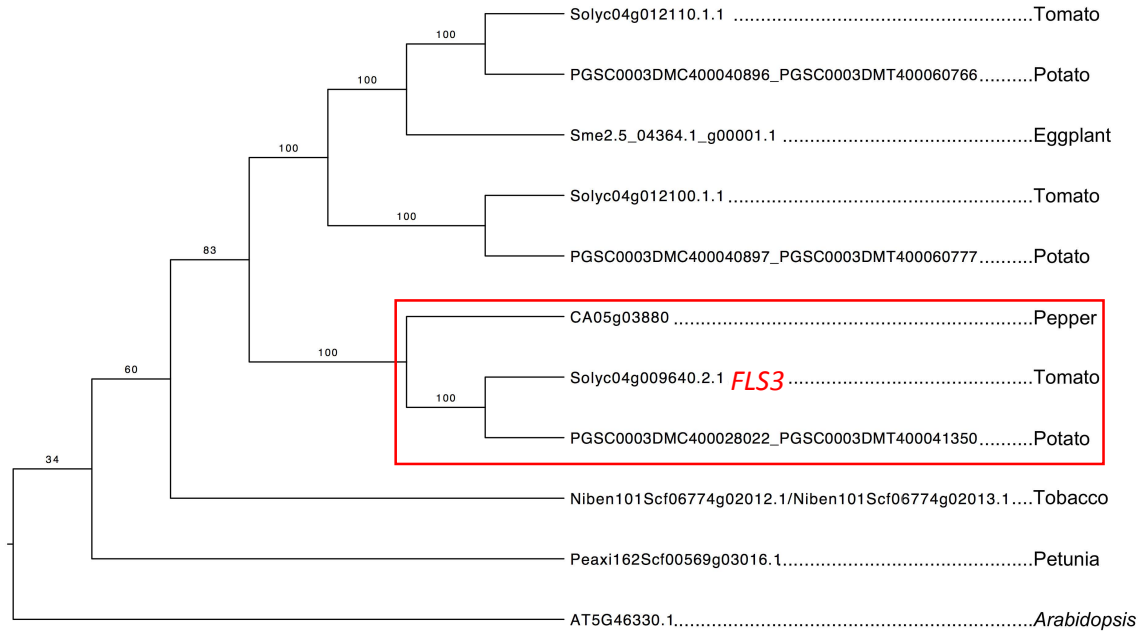

c

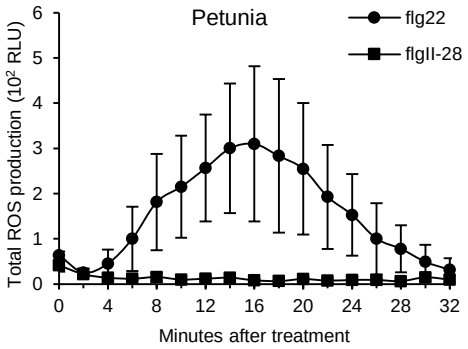

d

Species	Common Name	flg22 response	flgII-28 response	Ref.
Solanum lycopersicum	Tomato	+	+	11
Solanum tuberosum	Potato	+	+	12
Solanum melongena	Eggplant	+	?	12
Capsicum annum	Pepper	+	+	12
Nicotiana benthamiana	Wild tobacco	+	-	Fig. 3b
Petunia axillaris	Petunia	+	-	ED Fig.4c
Arabidopsis thaliana	Arabidopsis	+	-	12

Extended Data Figure 4. FLS3 functional domains and phylogenetic analysis. a, Amino acid changes found in *fls3* alleles are bold and underlined, and details provided in grey boxes. The K877Q amino acid substitution which is expected to interfere with kinase activity[19] is indicated. The kinase catalytic site shows that FLS3 is a non-RD kinase as it has the residues CD[18]. Dots serve as placeholders to facilitate demonstration of the conserved residues in the aligned LRR repeats. Modeled after Robatzek[69]. **b,** Phylogenetic analysis of *FLS3* and homologs from Solanaceous species. Branches are annotated with bootstrap support (100 replicates). Gene identifiers correspond to the following species: *Solanum lycopersicum* 'Heinz1706' (Tomato) - *Solyc04g012110.1.1*, *Solyc04g012100.1.1*, *Solyc04g009640.2.1*; *Solanum tuberosum* (Potato) - *PGSC0003DMC400040896_PGSC0003DMT400060766*, *PGSC0003DMC400040897_PGSC0003DMT400060777*, *PGSC0003DMC400028022_PGSC0003DMT400041350*; *Solanum melongena* (Eggplant) - *Sme2.5_04364.1_g00001.1; Capsicum annum* (Pepper) - *CA05g03880*; *Nicotiana benthamiana* (Wild tobacco) – *Niben101Scf06774g02012.1*/*Niben101Scf06774g02013.1; Petunia axillaris* (Petunia) - *Peaxi162Scf00569g03016.1; Arabidopsis thaliana* (Arabidopsis) – *AT5G46330.1.* The homolog in *N. benthamiana* is predicted as two gene models, but is likely a mis-annotation. The box indicates *FLS3* and its predicted orthologs. **c,** Oxidative burst produced by *Petunia axillaris* leaves treated with 100 nM flg22 or flgII-28 and measured in relative light units (RLU). Results shown are means ± s.d. (n = 4 plants). **d,** Summary of response to flg22 or flgII-28 treatment in all plant species tested. (+) indicates sensitivity to peptide treatment while (–) indicates insensitivity.

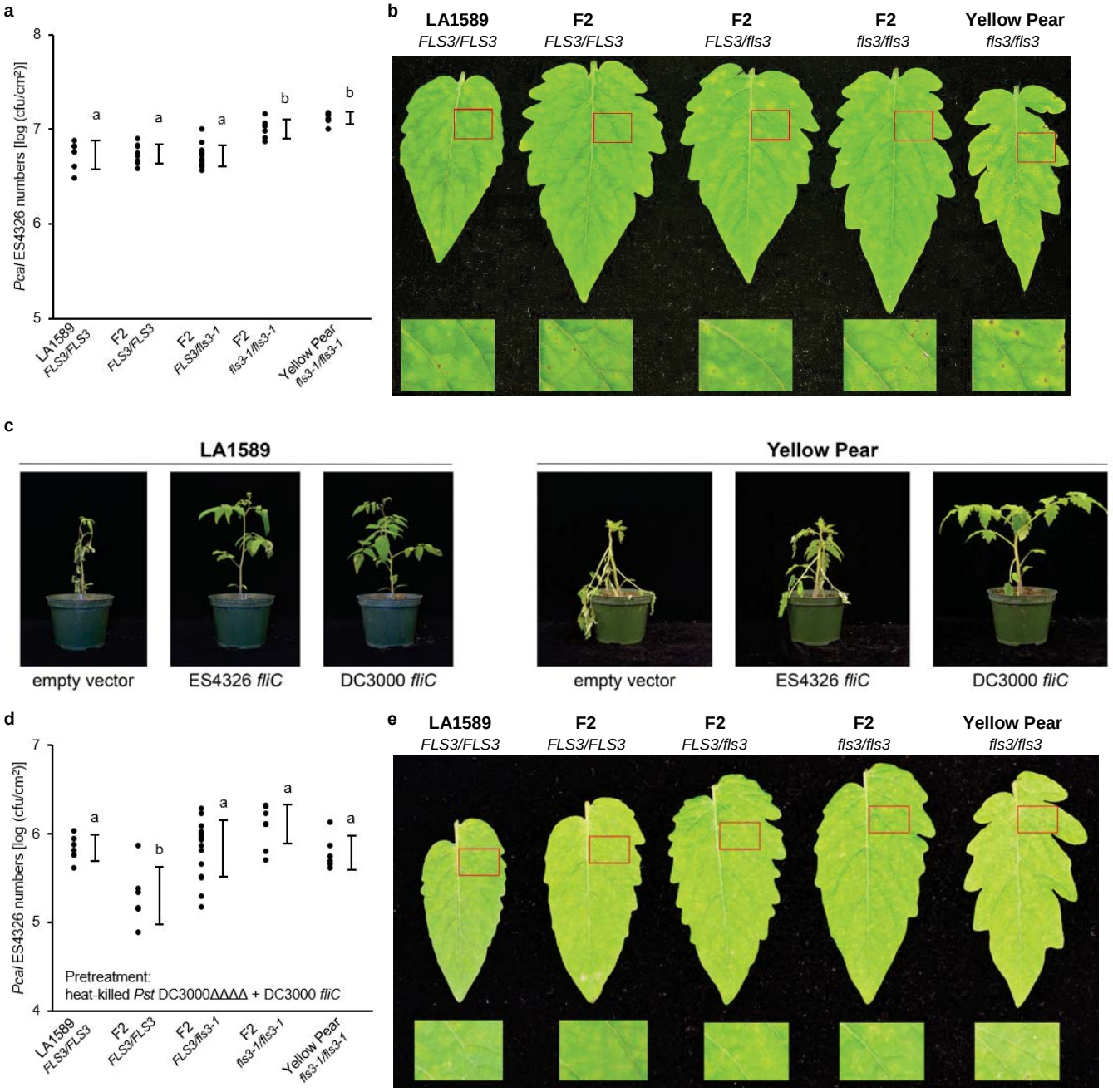

Extended Data Figure 5. *FLS3* is associated with enhanced resistance to bacterial infection. a, Bacterial populations of *Pcal* ES4326 (cfu/cm^2) were measured from F2 plants segregating for *FLS3* or *fls3-1*. Plants were infiltrated with bacterial suspensions of 3 x 10^4 cfu/mL and bacterial populations were measured 3 days after infiltration. Results shown are the individual values from each plant and s.d. (LA1589, $n = 6$; *FLS3/FLS3*, $n = 8$; *FLS3/fls3-1*, $n = 15$; *fls3-1/fls3-1*, $n = 6$; Yellow Pear, $n = 6$). Different letters indicate significant differences using Tukey-Kramer HSD test ($P < 0.05$) and similar but not always statistically significant results were obtained in five independent experiments. **b,** Representative

plants infiltrated as described in (**a**) except except *Pcal* ES4326 was inoculated at 1 x 10^5 cfu/mL, and photos were taken 4 days after bacterial infiltration. **c,** Representative plants infiltrated as described in Fig. 2c except *Pst* DC3000Δ*avrPto*Δ*avrPtoB*Δ*hopQ1-1*Δ*fliC* (DC3000ΔΔΔΔ) was inoculated at 1 x 10^5 cfu/ mL. Photos of LA1589 and Yellow Pear plants were taken 4 or 3 days after bacterial infiltration, respectively. **d,** Bacterial populations of *Pcal* ES4326 (cfu/cm^2) were measured from F2 plants segregating for *FLS3* or *fls3-1*. Plants were first infiltrated with bacterial suspensions of 10^8 cfu/mL of heat-killed *Pst* DC3000ΔΔΔΔ complemented with DC3000 *fliC*, and 16 hours later were inoculated with bacterial suspensions of *Pcal* ES4326 at 5 x 10^4 cfu/mL. Bacterial populations were measured 2 days after bacterial infiltration. Results shown are the individual values from each plant and s.d. (LA1589, $n = 6$; *FLS3/FLS3*, $n = 6$; *FLS3/fls3-1*, $n = 16$; *fls3-1/fls3-1*, $n = 7$; Yellow Pear, $n = 9$). Different letters indicate significant differences using Tukey-Kramer HSD test ($P < 0.05$); however, no consistent differences were observed between three independent experiments. **e,** Representative plants infiltrated as described in (**d**) except *Pcal* ES4326 was inoculated at 1 x 10^5 cfu/mL, and photos were taken 4 days after bacterial infiltration.

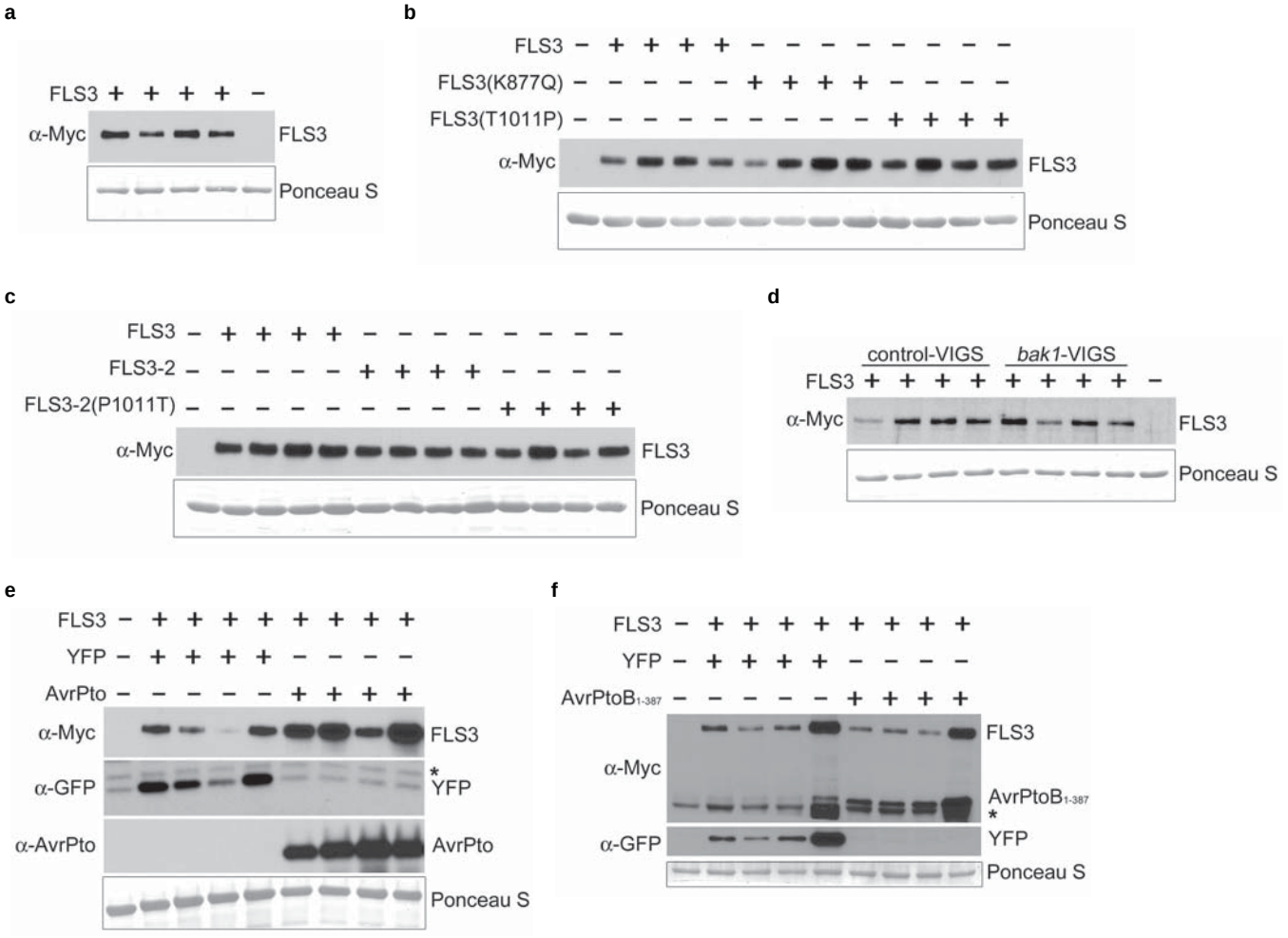

Extended Data Figure 6. Immunoblot analysis of *Agrobacterium*-mediated transient protein expression in *N. benthamiana* leaves. Except where indicated otherwise, each immunoblot depicts four plant samples per construct or construct combination from one experiment. Untransformed (-) controls are included to show non-specific antibody labeling. **a**, Protein levels of FLS3-Myc corresponding to Figure 3b. Top panel: immunoblotting with anti-Myc antibodies. Bottom panel: Ponceau S staining to demonstrate equal loading. **b**, Protein levels of FLS3-Myc and FLS3 kinase domain mutants FLS3(K877Q)-Myc and FLS3(T1011P)-Myc corresponding to Figure 3c. Top panel: immunoblotting with anti-Myc antibodies. Bottom panel: Ponceau S staining to demonstrate equal loading. **c**, Protein levels of FLS3-Myc, FLS3-2-Myc and FLS3-2(P1011T)-Myc corresponding to Figure 3d. Top panel: immunoblotting with anti-Myc antibodies. Bottom panel: Ponceau S staining to demonstrate equal loading. **d**, Protein levels of FLS3-Myc corresponding to Figure 5a. Top panel: immunoblotting with anti-

Myc antibodies. Bottom panel: Ponceau S staining to demonstrate equal loading. **e**, Protein levels of FLS3-Myc, YFP-Myc and AvrPto-Myc corresponding to Figure 4c. From top panel (1) to bottom panel (4). Panel 1: immunoblotting with anti-Myc antibodies. Panel 2: immunoblotting with anti-GFP antibodies. Panel 3: immunoblotting with anti-AvrPto antibodies. Panel 4: Ponceau S staining to demonstrate equal loading. **f**, Protein levels of FLS3-Myc, YFP-Myc and $AvrPtoB_{1-387}$-Myc corresponding to Figure 4d. From top panel (1) to bottom panel (3). Panel 1: immunoblotting with anti-Myc antibodies. Panel 2: immunoblotting with anti-GFP antibodies. Panel 3: Ponceau S staining to demonstrate equal loading. Asterisk indicates non-specific labeling.

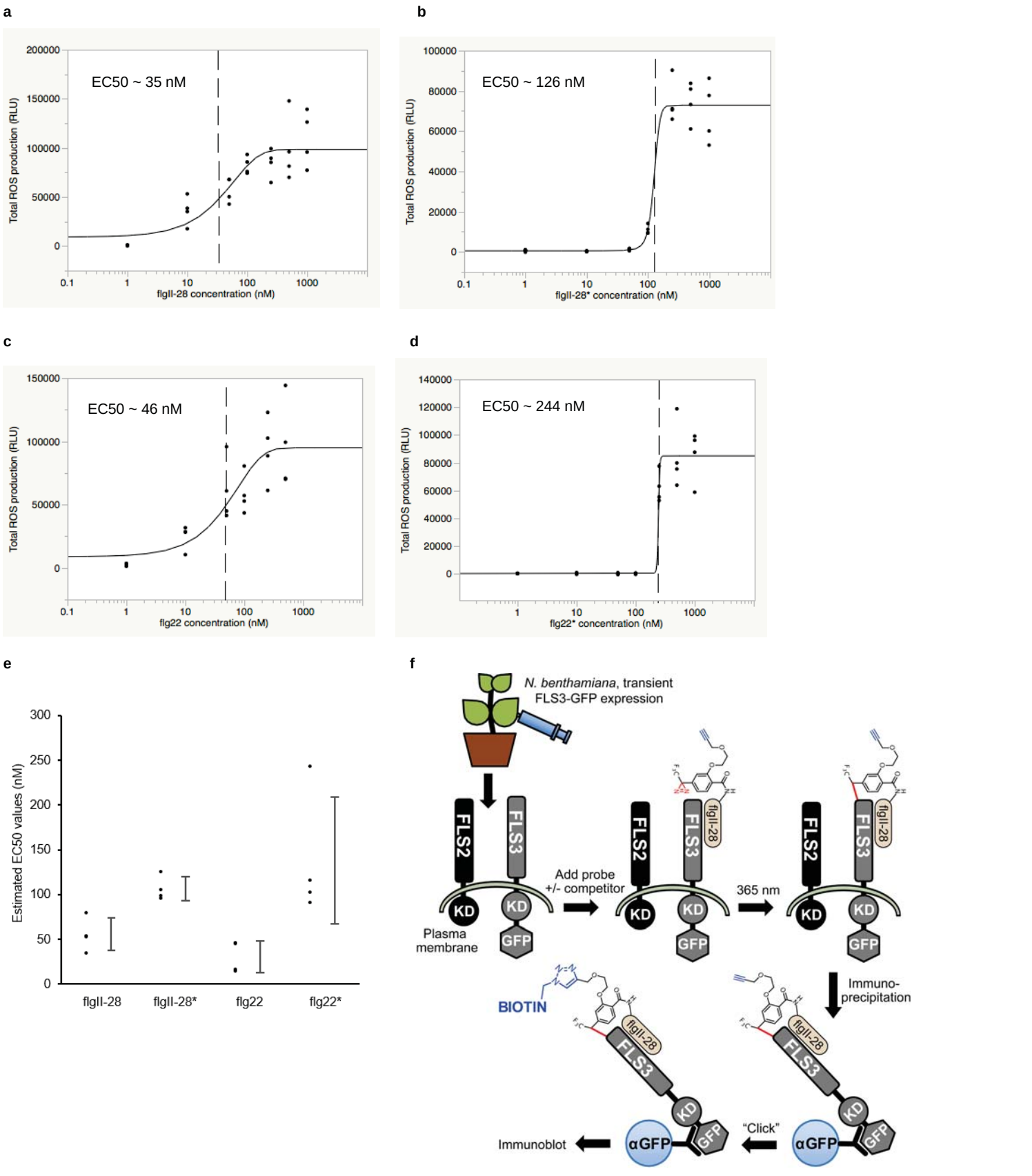
a
EC50 ~ 35 nM
Total ROS production (RLU)
flgII-28 concentration (nM)
b
EC50 ~ 126 nM
Total ROS production (RLU)
flgII-28* concentration (nM)
c
EC50 ~ 46 nM
Total ROS production (RLU)
flg22 concentration (nM)
d
EC50 ~ 244 nM
Total ROS production (RLU)
flg22* concentration (nM)
e
Estimated EC50 values (nM)
flgII-28
flgII-28*
flg22
flg22*
f
N. benthamiana, transient
FLS3-GFP expression
FLS2
FLS3
KD
GFP
Plasma
membrane
Add probe
+/- competitor
flgII-28
365 nm
Immuno-
precipitation
BIOTIN
"Click"
αGFP
Immunoblot

Extended Data Figure 7. Peptide affinities and experimental scheme for binding experiments. a-d, EC50 predictive modeling curves used to estimate EC50 values in (**e**). Oxidative burst produced by Rio Grande tomato leaves treated with concentrations of flgII-28 and flg22 peptides or probes ranging from 1 to 1000 nM and measured in relative light units (RLU). Data points shown are individual total ROS production for each concentration (n = 4 plants). The fitted curves were predicted by the JMP software using the non-linear logistic 4p formula as described previously[71] with predicted EC50 value indicated by the vertical dashed line. Similar results were obtained in four independent experiments. **e,** Estimated EC50 for flgII-28 and flg22 peptides or probes using values obtained in four independent experiments as described above. Data points shown are the inferred EC50 values and s.d. (n = 4). **f,** Experimental scheme for binding experiments. Plasma membrane-enriched microsomes were harvested from *N. benthamiana* leaf tissue expressing FLS3-GFP (or FLS2-GFP), incubated with indicated concentrations of either peptide-probes (flgII-28* or flg22*) or peptide-probes with unmodified competitor peptides (flgII-28 or flg22) followed by UV-irradiation at 365 nm. Immunoprecipitated FLS3-GFP was used in a "click" reaction with biotin azide and analyzed by immunoblotting.

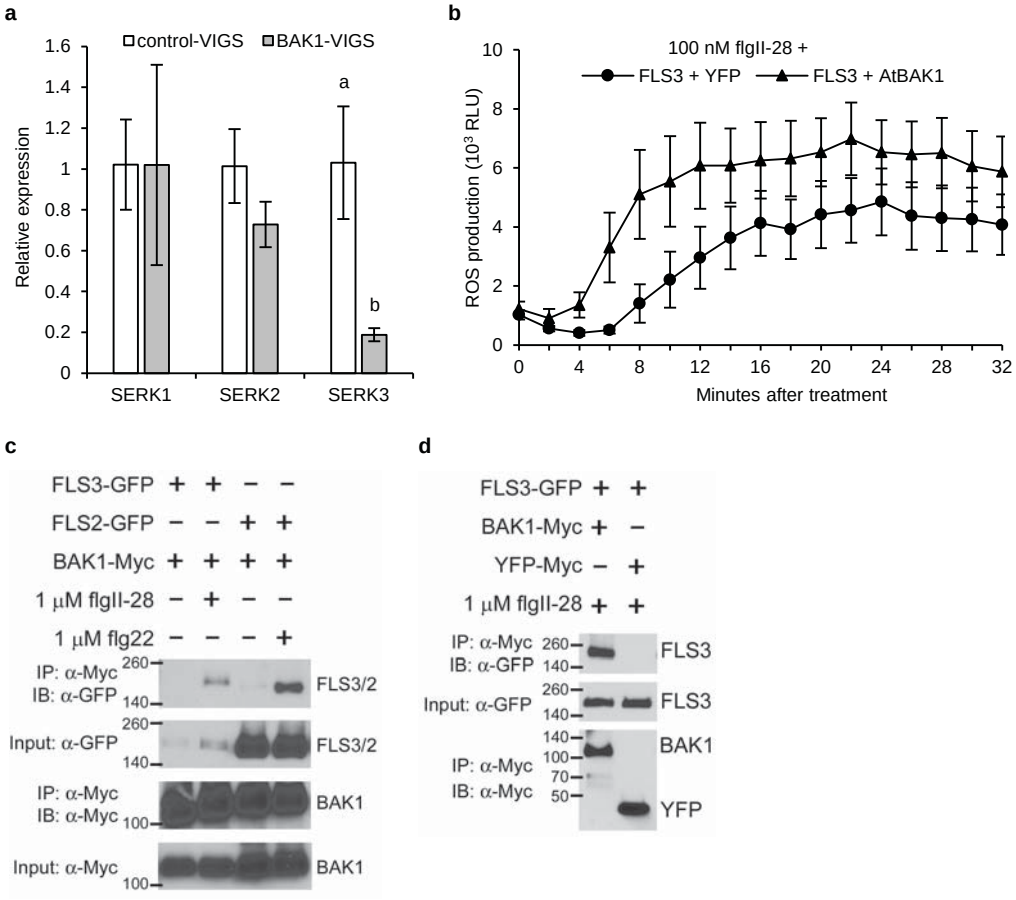

Extended Data Figure 8. FLS3 signaling requires BAK1 and FLS3 associates with BAK1 *in vivo* in a flgII-28-dependent manner. a, Relative expression of different *SERK* genes in *N. benthamiana* leaves silenced for *BAK1* or a control gene by VIGS was determined using quantitative real-time reverse transcription PCR (qRT-PCR) with primers described previously[66]. The relative expression of the *SERK* genes was normalized using *NbUbq*. Results shown are the means ± s.d. (n = 4 plants per construct). Similar results were obtained in two independent experiments; however, while the *SERK3* transcript was significantly different in both experiments, the reduction of *SERK2* transcript was not significantly reduced in the second experiment. Different letters indicate significant differences using Student's t-test ($P < 0.05$). **b**, Oxidative burst produced by *N. benthamiana* leaves silenced for *BAK1* by VIGS, expressing FLS3 in combination with either YFP or AtBak1 and treated with 100 nM flgII-28, and measured in relative light units (RLU). Both construct combinations were expressed on the same leaves. Results shown are means ± s.d. (n = 4 plants per experiment). **c,** FLS3 can be found in a complex with BAK1

specifically after treatment with flgII-28. *N. benthamiana* leaves expressing either FLS3-GFP or FLS2-GFP in combination with AtBAK1-Myc, and treated with buffer alone, 1 μM flgII-28, or 1 μM flg22 for 2 minutes before harvesting, were used for immunprecipitation using anti-c-Myc affinity resin. Both FLS3 and FLS2 are pulled down with BAK1 after treatment with 1 μM flgII-28 or flg22, respectively, but not buffer alone (top panel) though both samples contain FLS3-GFP or FLS2-GFP (middle panel), and BAK1-Myc is also present (bottom panels). **d,** FLS3 can specifically associate with BAK1. *N. benthamiana* leaves expressing FLS3-GFP in combination with either AtBAK1-Myc or YFP-Myc, and treated for 10 minutes with 1 μM flgII-28 before harvesting, were used for immunprecipitation using anti-c-Myc affinity resin. FLS3 is pulled down with BAK1 but not with YFP (top panel) though both samples contain FLS3-GFP (middle panel), and immunoprecipitated BAK1-Myc and YFP-Myc are also present (bottom panel). For parts **b-d**, similar results were obtained in three independent experiments.